VON KARMAN INSTITUTE FOR FLUID DYNAMICS
CHAUSSEE DE WATERLOO, 72
B - 1640 RHODE SAINT GENESE, BELGIUM

PR 1982-24 JUNE 1982

INVESTIGATION OF HEAT TRANSFER RATES ON A FILM COOLED FLAT PLATE WITH ONE AND TWO ROWS OF INJECTION HOLES

M. PEZZANI

SUPERVISORS : P.M. LIGRANI
C. CAMCI

TABLE OF CONTENTS

ABSTRACT

Results from an investigation of heat transfer ratio on a film cooled flat plate with one and two rows of injection are presented. Data are given for different blowing ratios at two different coolant temperatures. h/h_0 distributions are presented for both cases. Experimental distributions of estimated values of film cooling effectiveness are presented for the double row case and compared with results from the literature.

LIST OF SYMBOLS

A	area	m^2
C_D	discharge coefficient	
C_p	specific heat at constant pressure	(J/kgK)
d, D	orifice throat diameter	mm
h	heat transfer coefficient, $q/(T_{0,\infty}-T_w)$	(J/sec°K/m²)
h_f	film cooling heat transfer coefficient, $q(T_{a_w}-T_w)$	(J/sec°K/m²)
h_0	heat transfer coefficient without film cooling, $q/(T_{0,\infty}-T_w)$	(J/sec°K/m²)
m	isentropic blowing ratio $(\rho_c U_c)_i/\rho_\infty U_\infty$	-
M	Mach number	-
P	pressure	bar
R	gas constant	(J/kg°K)
$\dot{q}''_0$	wall heat flux without film injection	W/cm^2
$\dot{q}''_f$	wall heat flux with film injection	W/cm^2
T	temperature	°K
St	Stanton number, $h/\rho U_\infty C_p$	-
Re	Reynolds number, $U_\infty \kappa/\nu$	-
U	velocity	m/sec
x	distance for origin of turbulent boundary layer	m
η_{ad}	adiabatic film cooling effectiveness	-
θ	one dimensional coolant temperature, $(T_{0,\infty}-T_{0,c})/(T_{0,\infty}-T_w)$	-
θ_0	value of θ when $h/h_0 = 0$	-
μ	absolute viscosity	(kg/msec)

Re_c	Reynolds number for coolant flow $\frac{\rho_c u_c \pi D}{6\mu_c}$	-
ξ	correlating parameter, see reference 8	-
Pr	Prandtl number, $C_p\mu/k$	-
I	momentum flux ratio, $\rho_c U_c^2/\rho_\infty U_\infty^2$	-
α	pressure ratio, $P_{0,c}/P_{0,\infty}$	-
γ	specific heat ratio	-
ρ	density	(kg/m^3)

<u>Subscripts</u>

aw	adiabatic wall
c	coolant
b	bleeds
w	wall
0	total
∞	free stream
is	isentropic
m	main sonic orifice
i	injection
a	actual
up	upstream of sonic orifice, total conditions

LIST OF FIGURES

TABLE I

1. INTRODUCTION

The turbine entry temperature plays an important role in the improvement of gas turbines efficiency. Since the 1960's a way to improve that efficiency has been to internally cool the first stages of the turbine. Since about 1970 the air used to internally cool the blade has been further employed to provide a protective film on the blade surface and therefore allows a further increase in the turbine inlet temperature. The effectiveness of the protective film depends on the behaviour of the thermal and hydrodynamic boundary layer as modified by the coolant jet and by real turbine effects such as variable wall temperature, curvature, rotation, free stream turbulence, secondary flows, surface roughness, acceleration, deceleration and unsteady effects. Complete experimental simulations of these and other effects require testing on a real turbine rig.

To allow understanding of such effects, tests are required in an experimental facility and on an experimental model which allow the researcher to quantify the influence of an individual effect without the influence of others. Examples of this approach can be found in the work of researchers at Stanford University and at the University of Minnesota. Researchers at the former institution aim at obtaining the evaluation of the film cooling effects through the measurement of heat transfer coefficients whereas at the latter, measurements of the adiabatic wall temperature are made and often presented adimensionalized as the adiabatic film cooling effectiveness η_{AD}, where :

$$\eta_{AD} = \frac{T_{AD}-T_{0,\infty}}{T_{0,c}-T_{0,\infty}} \tag{1}$$

The objective of the present study is to evaluate the film cooling effectiveness in a transient facility, under isothermal wall conditions and compare it with measurements of the adiabatic film cooling effectiveness obtained from steady state facilities. In transient facilities, one can only indirectly evaluate the film cooling effectiveness and thus differences may exist from steady state measurements. The second aim of the study is to obtain film cooling results at conditions which closely simulate those in a gas turbine , ($Ma, Re, T_W/T_\infty/T_C$).

2. PREVIOUS WORK

In 1971, Goldstein (Ref. 1) presented a detailed review and assessment of two dimensional and three dimensional film cooling techniques and investigations. Most of these investigations simulate unrealistic gas turbine situations such as film heating, small temperature ratios, incompressible flow. Liess (Ref. 2) in 1973, correctly simulated Mach number and Reynolds numbers, but did not scale the temperature ratios. More recently, new transient techniques which allow a correct simulation of gas turbine conditions have been presented in references 3, 4, 14 and 15.

E.R.G. Eckert, discussing the results from a paper by D.E. Metzger, (Ref. 5) proposed a linear relationship between the classical heat transfer coefficient, h, and a non dimensional coolant temperature, θ. Ville et al. (Ref. 6) experimentally confirmed this linear relationship in compressible flow with an isothermal wall, while Ville et al. (Ref. 7) confirmed it by varying both the wall and injection temperature and further demonstrated the capability of short duration facilities to provide useful and realistic heat transfer information under well simulated gas turbine conditions.

If there is no injection, the heat transfer from the gas to the wall is described by the equation

$$q_0'' = h_0\left(T_{0,\infty} - T_w\right) \qquad (2)$$

where $T_{0,\infty}$ is the total temperature of the gas. If there is injection, the heat transfer to the wall is given by :

$$q_f'' = h_f\left(T_{aw} - T_w\right) \qquad (3)$$

where T_{aw} is the adiabatic wall temperature, i.e., the temperature the flow would attain if the wall was adiabatic. h_f is the heat transfer coefficient associated with injection at θ=0.

An alternative way to express the heat flux with injection is by means of the main stream temperature and a heat transfer coefficient, h, which alone, accounts for injection effects :

$$q_f'' = h\left(T_{0,\infty}-T_w\right) \tag{4}$$

From the equations (3) and (1) one can obtain :

$$\dot{q}_f'' = h_f\left(T_{0,\infty}-T_w\right)\left(1-\eta_{ad}\theta\right) \tag{5}$$

where θ is a non dimensionalization of the coolant flow temperature with respect to the main stream total temperature and wall temperature, as given by :

$$\theta = \frac{T_{0,\infty}-T_{0,c}}{T_{0,\infty}-T_w} \tag{6}$$

From equations (4) and (5),

$$h = h_f\left(1-\eta_{ad}\theta\right) \tag{7}$$

which defines a linear relationship between h and θ (Fig. 1). From (7), for h ≑ 0 one obtains that :

$$\theta_0 = \frac{1}{\eta_{ad}} = \frac{T_{0,\infty}-T_{0,c}}{T_{0,\infty}-T_w} \tag{8}$$

and thus, by directly extrapolating the line h versus θ to the h = 0 abscissa one obtains an indication of η_{ad}. For θ = 0, one may also obtain :

$$h = h_f \tag{9}$$

Jabbari & Goldstein (Ref. 8) indicate that, under incompressible flow conditions and small temperature differences, the spanwise averaged heat transfer coefficient with injection, $\bar{h}_f$, is within a few percent of that without injection h_0 at low blowing rates. h_f increases fast as the blowing rate increases above unity in tests on a flat plate with two rows of injection. Yoshida and Goldstein (Ref. 9) indicate that a different influence exists from turbulent or laminar flows that can, at least qualitatively be explained in terms of different transport mechanisms. Their study was made using a flat plate with one row of film cooling holes.

In order to evaluate η_{ad} in a transient facility, one must first non dimensionlize equation (7), with the heat transfer coefficient with no injection, h_0, to obtain :

$$h/h_0 = h_f/h_0\left(1-\eta_{ad}\theta\right) \tag{10}$$

For $\theta = 0$, this then gives

$$h = h_f \tag{11}$$

and, under certain circumstances (Ref. 8) :

$$h_f = h_0 \tag{12}$$

Thus, once the linearity of h versus θ has been obtained experimentally η_{AD} may be evaluated using only one experimental point at $\theta \approx 1$ for example, along with equations (10)-(12) if all of the above assumptions are valid.

3. EXPERIMENTAL TECHNIQUES

The reported tests were conducted in the CT-2 facility at the VKI. This facility, shown in figure 2, is a light piston isentropic compression tube rig able to simulate realistic gas turbine conditions. A full description of the facility and its operation is given in reference 7.

3.1 Models

Two models were used during the testing : one shown in figure 3, cooled using one row of 51 injection holes, the other cooled by two rows of 101 injection holes. For both models, the holes had a diameter of 0.5 mm and were spaced 3D apart and angled 35° with the horizontal.
Test conditions were as follows : total free stream temperature of 400°K, total pressure of 2.90 bar, no pressure gradient along the test section, free stream Mach number of .64. Figure 4 shows the plenum chamber of the single row model whereas figure 5 shows that of the double row model. The latter shows two sonic bleeds added to decrease the flushing time of the plenum chamber to decrease the establishment time of the secondary flow on the flat plate.

3.2 Injection system

During the testing of both models two different injection systems were used, shown in figures 6a and 6b. Configuration a was used early with the single row model. Its main disadvantage is the slow establishment of the secondary flow due essentially to the low mass flow rates involved; to overcome this disadvantage, configuration b was used; its advantage over configuration a is the availability, at the beginning of the injection, of a large mass flow rate which is afterwards decreased to the wanted value by closing the by-pass valve shown in the figure. An optimization of the injection process may be obtained only when the plenum chamber and injection system are both being considered. In this respect, the injection system of figure 6a together with the plenum chamber of figure 5 has given the best results in terms of speed establishment of the secondary flow. What is said above, is confirmed by the traces of the plenum chamber versus time, for three different combinations shown in figures 7a,b,c.

Figure 7a shows the typical problem encountered with the configuration of figure 6a when matched to the plenum chamber of figure 4; that is, the difficulty in keeping a constant rate of injection during the experiment. Figure 7b presents a typical trace for the configuration of figure 6b. Figure 7c shows what may be obtained by matching the injection system of figure 6a with the plenum chamber of figure 5 : the injection is established in a very short time, typically less than 80 msecs, and is steady during the whole experimental sampling time.

3.3 Heat transfer measurement

For both models 18 thin film heat gages were placed downstream of the injection location. The transversal length of the heat gages was 4.5 mm for the single row model and 12.0 mm for the double row model : this change was dictated by the need to increase the number of holes covered by the heat gages in the transversal direction. The large span gages give a better measurement of the average heat flux, especially when large spanwise variations exist just downstream of the injection holes. Heat flux measurement techniques using thin film heat gages are fully described in references 13, 14 and 15.

4. RESULTS

Figure 8 shows the convective heat transfer on a flat plate without injection as Stanton number versus Reynolds number. The agreement with the correlation suggested by Kays (Ref. 12), for the case of an isothermal wall is excellent. The certainty is 9.6% at a confidence level of 95%. The experimental results agree with the proposed correlation within 5% and repeatability is 2%. The presence of a tripping wire on the flat plate surface at a known distance from the leading edge allows the calculation, by means of standard correlations (Ref. 11), of the origin of the downstream coordinate, needed to properly evaluate the Reynolds number. This also allows the control of the value of the boundary layer displacement thickness over the injection section so that it is comparable with values used in other reported work. The value of δ_1/D in the present study is 0.16 at the location of the film cooling holes. The base line result confirms the validity of the experimental technique and the capability of a transient facility to produce results comparable with those obtained on a steady state facility.

If one chooses a downstream location and assumes the value of the heat flux at that location as constant with the downstream distance then one obtains the constant heat flux distribution of St versus Re. This is shown in figure 9 together with the theoretical correlation for the case of constant heat flux by Kays (Ref. 12). Figure 10 compares St versus Re distributions for constant wall temperature and constant heat flux walls, and shows that the St distribution for a constant wall heat flux boundary condition depends on the choice of the downstream location at which its value is taken.

The wall temperature is not constant in the downstream direction after a test has begun, as shown by an analysis of the wall temperature versus time signals, an example of which is shown in figure 11. Figure 12 shows the variation of the wall temperature with downstream distance, obtained by sampling the traces of signals from thin film gages at 450 msecs. The resulting experimental St versus Re distribution, shown in figure 13, follows the same trend as the one for an isothermal wall case, and St values are lower than for isothermal boundary conditions.

The linearity of the energy equation, as shown by Jones (Ref. 10) can be used also in realistic gas turbine conditions. Therefore, the method of superposition can be applied, in the present study, to find heat transfer solutions for the boundary layer to account for an arbitrary variation of the wall temperature. Because the present work was carried out in a transient facility, a modified version of Kays & Crawford (Ref. 12) superposition method was used : the first step change of the approximation of the temperature wall distribution is taken as positive, contrary to what Kays & Crawford suggest (Ref. 12) in order to take into account the transient situation in which the tests were performed. Figure 14 shows the approximation used and the resulting St versus Re distribution compared with the experimental curve from figure 13. The temperature versus distance distribution was chosen so that the St versus Re superposition results provided a good fit to experimental results.

4.1 Single row results

Figures 15 and 16 show results for injection at ambient temperature through a single row of injection, plotted as h/h_0 versus x/D. The trends shown by these results are consistent with a physical explanation of the phenomenon, although the absolute values are higher than expected. Consider first the parts of figures 15 and 16 for values of x/D less than 35, an increasing value of m results in a decrease of h/h_0 for values of m less than .71. Above this value h/h_0 increases probably due to too strong blowing into the boundary layer. The second part of figures 15 and 16 is affected by the thickening of the boundary layer due to the mass injected. Such results are in agreement with published work (Ref. 9) on similar models for a comparable range of blowing ratios. However, the results of 15 and 16 disagree in magnitude with published results. It is the belief of the author that the main reason for disagreement in magnitude is the very short transversal length of the heat gages on the single row model. The span of only two injection holes was covered by the heat gages. The effect of film-cooling, especially at downstream distances near the injection location, is then diminished due to spanwise averaging by the heat gages.

4.2 Double row injection results

Figures 17 and 18 show results of injection at ambient temperature $T_{0,c}$ = 290°K with the double row model, whereas figures 19 and 20 show results of injection at temperatures around a $T_{0,c}$ of 314°K with the same model. Table I presents the coolant variables for the same tests as obtained using the computer program included in Appendix II. The reduction procedure is presented in Appendix I.

When compared at the same m and x/D, the results for the hot injection are higher than those when the injection temperature was near ambient. The ambient tests also show a region at small x/D where a complicated interaction takes place. Downstream of this region, h/h_0 variations with m at given x/D follow more consistent trends. For the tests at the higher temperature, the film cooling effect retains its influence for a shorter distance after which the trends repeat those of the tests at ambient temperature.

Figures 21 and 22 show the degree of correlation between the measured results of the present work and two dimensional models (Ref. 1). Figures 21 and 22 show the film cooling effectiveness, η_{AD} versus a correlating parameter, ξ, where ξ is defined using

$$\xi = \left[\left(x+1.909D\right) / m \frac{\pi D}{6}\right] \left(Re_c \frac{\mu_c}{\mu_\infty}\right)^{-0.25}$$

$$\text{where } Re_c = \frac{\rho_c u_c \pi D}{6\mu_c}$$

Values of $\bar{\eta}_{ad}$, presented in figure 21 are evaluated using equation (12) and an additional h/h_0 data point determined from an average of hot and ambient measurement results. In figure 22, $\bar{\eta}_{AD}$ was determined by extrapolating a line, from $\frac{h_f}{h} = 1$ at $\theta = 0$, and $\frac{h}{h_0}$ at $\theta \approx 1$ to the $h = 0$ intercept. It is worth noting that for both evaluations of η_{ad}, the agreement improves for values of ξ greater than 10. Such behaviour is consistent with experimental results obtained by Jabbari et al (Ref. 8) on a similar model, but in an incompressible flow situation where small temperature differences existed.

5. CONCLUSIONS

An experimental program has been carried out to investigate the heat transfer to a flat plate with one and two rows of injection holes. Ma, Re and wall/gas/coolant temperature ratios were chosen to simulate realistic gas turbine conditions.

Single row injection results show similar trends, but large quantitative differences with results from published literature. Estimated values of $\bar{\eta}_{ad}$ for two row injection cases show a good degree of agreement with two dimensional film cooling models and with experimental results obtained under incompressible flow conditions.

REFERENCES

1. GOLDSTEIN, R.J.: Film cooling. In:
   Advances in Heat Transfer, Ed. Irvine,
   Academic Press, Vol. 7, 1971, pp 321-379.

2. LIESS, C.: Film cooling with ejection from a row of inclined circular holes - An experimental study for the application to turbine blades.
   VKI TN 97, March 1973.

3. SCHULTZ, D.L. & JONES, T.V.: Heat transfer measurements in short duration hypersonic facilities.
   AGARDograph 165, 1973.

4. OLDFIELD, M.L.G.; JONES, T.V.; SCHULTZ, D.L.: On-line computer for transient cascade instrumentation.
   IEEE Trans. on Aerospace and Electronic Systems,
   Vol. AES-14, No. 5, 1978.

5. METZGER, D.E.; CARPER, H.J.; SWANK, L.R.: Heat transfer with film cooling near nontangential injection slots.
   ASME Trans., Series A - J. Engineering for Power,
   Vol. 90, No. 2, April 1968, pp 157-163.

6. VILLE, J.P. & RICHARDS, B.E.: The measurements of film cooling effectiveness on turbine components in short duration wind tunnels. In:
   High Temperature Problems in Gas Turbine Engines,
   AGARD CP 229, Paper 34, 1977.

7. VILLE, J.P.; CUNAT, D.; RICHARDS, B.E.: The measurement of film cooling effectiveness in short duration wind tunnels.
   VKI TN 127, December 1978.

8. JABBARI, M.Y. & GOLDSTEIN, R.J.: Adiabatic wall temperature and heat transfer downstream of injection through two rows of holes.
   ASME Trans., Series A - J. Engineering for Power,
   Vol. 100, No. 2, April 1978, pp 303-307.

9. GOLDSTEIN, R.J. & YOSHIDA, T.: The influence of a laminar boundary layer and laminar injection on film cooling performance.
   ASME Paper 81-HT-38, April 1981.

10. LOFTUS, P.J. & JONES, J.V.: The effect of temperature ratios on the film cooling process. In:
    Film Cooling and Turbine Blade Heat Transfer,
    VKI LS 1982-02, February 22-26, 1982.

11. SCHLICHTING, H.: Boundary layer theory. Seventh edition.
    McGraw Hill, 1979, pp 536-542.

12. KAYS, W.M. & CRAWFORD; M.: Convective heat and mass transfer.
McGraw-Hill, 1980.

13. LIGRANI, P.M.; CAMCI, C.; GRADY, M.S.: Thin film heat transfer gage construction and measurement details.
VKI IN 72, March 1982.

14. CAMCI, C.; LIGRANI, P.M.; HAY, M.: Investigation of heat transfer rates on a film cooled plate with and without a pressure gradient.
VKI IN 68, July 1981.

15. LIGRANI, P.M. & BREUGELMANS, F.A.E.: Turbine blade-cooling research at the von Karman Institute for Fluid Dynamics.
Fifth International Symposium on Air Breathing Engines, Bangalore, India, February 1981. Also:
VKI Preprint 1981-06.

APPENDIX I - INJECTION DATA REDUCTION PROCEDURE

The procedure, hereafter described, calculates relevant coolant variables once the free stream, plenum, upstream of the main sonic orifice conditions are known, from the experiment.

Inputs :

- Upstream orifice total pressure
- Upstream orifice total temperature
- Plenum chamber total pressure
- Plenum chamber total temperature
- Ambient pressure
- Free stream Mach number
- Free stream total temperature
- Free stream total pressure
- Discharge coefficient

Outputs :

- Free stream static pressure
- Free stream static temperature
- Free stream velocity
- Free stream density
- Coolant static density
- Coolant static temperature
- Coolant velocity
- Blowing ratio
- Momentum flux ratio
- Velocity ratio
- Density ratio
- Discharge coefficient

From :

$$T_\infty = T_{0,\infty}\left(1+\frac{M_\infty^2}{5}\right)^{-1} \qquad (1)$$

$$P_\infty = P_{0,\infty}\left(1+\frac{M_\infty^2}{5}\right)^{-7/2} \qquad (2)$$

the static temperature and pressure are obtained; density is obtained from :

$$\rho_\infty = \frac{P_\infty}{RT_\infty} \qquad (3)$$

whereas :

$$u_\infty = M_\infty\sqrt{\gamma RT_\infty} \qquad (4)$$

The isentropic mass flux ratio, m_{is}, is calculated through :

$$m_{is} = \alpha^{2/7} \times \left(\frac{T_{0,\infty}}{T_{0,c}}\right)^{0.5} \sqrt{\frac{1-\left(\alpha\,\dfrac{P_{0,\infty}}{P_{0,c}}\right)^{-2/7}}{1-\left(\dfrac{P_{0,\infty}}{P_{0,c}}\right)^{-2/7}}} \qquad (5)$$

and the isentropic mass flux, $\rho_c u_{c_{is}}$, is :

$$\rho_c u_{c_{is}} = m_{is} \times \rho_\infty u_\infty \qquad (6)$$

At this stage, if the main sonic orifice diameter is available the calculation proceeds as follows : the mass flow rate through the main orifice is given by :

$$\dot{m}_M = \pi \times 4.0424 \times 10^{-3} \times d^2(\text{mm}) \times \frac{P_{up}}{\sqrt{T_{up}}} \tag{7}$$

and the mass flow rate through the bleeds is

$$\dot{m}_B = \pi \times 4.0424 \times 10^{-3} \times d^2(\text{mm}) \times \frac{P_{0,c}}{\sqrt{T_{0,c}}} \tag{8}$$

so that the injected mass flow rate is :

$$\dot{m}_i = \dot{m}_M - 2\dot{m}_B \tag{9}$$

and the actual mass flux is equal to :

$$\rho_c u_{c_a} = \frac{\dot{m}_i}{A_i} \tag{10}$$

The discharge coefficient can then be evaluated as :

$$C_D = \frac{\rho_c u_{c_a}}{\rho_c u_{c_{is}}} \tag{11}$$

If the main sonic orifice diameter is not available, then one has to assume a value from the discharge coefficient and from that calculate the actual mass flux, as

$$\rho_c u_{c_a} = \rho_c u_{c_{is}} \times C_D \tag{12}$$

Figure 23 shows the degree of correlation between values of C_D obtained experimentally on the double row model and values calculated with equation (11), as explained above.

By assuming that the coolant static pressure is equal to the free stream static pressure at the injection location on the flat plate surface one can set up the following system of equations the solution of which gives the values of the remaining unknowns : ρ_c, u_c, T_c :

$$\rho_c = \frac{P_\infty}{RT_c} \tag{13}$$

$$T_{0,c} = T_c + \frac{u_c^2}{2C_p} \tag{14}$$

$$u_c \rho_c = (u_c \rho_c)_a \tag{15}$$

Appendix II contains the listing of the program INJ which carries out this procedure, together with the evaluation of the $1/\theta_0$ distribution along the lines explained in chapter 4.

APPENDIX II - DATA REDUCTION PROGRAM

```
C     THIS PROGRAM CALCULATES THE INJECTION FLOW PARAMETERS USING
C     EXPERIMENTAL DATA ON CT-2 FACILITY AT VKI.
C     OPTIONS AVAILABLE ARE:1)- CALCULATION THROUGH DISCHARGE COEFF-
C                               FICIENT AND PLENUM CHAMBER CONDITIONS
C                           2)- CALCULATION THROUGH MAIN CALIBRATED
C                               ORIFICE AND UPSTREAM ORIFICE CONDITIONS
C     USE OF THE LINEARITY OF THE H/HO VS THETA RELATIONSHIP ALLOWS
C     THE CALCULATION OF THE ADIABATIC FILM COOLING EFFECTIVENESS;
C     THREE OPTIONS ARE AVAILABLE:
C     1)- ONE POINT AVAILABLE ON THE H/HO VS THETA PLOT: ASSUME HF/HO=1 FOR THETA=0
C     2)- TWO POINTS   "         "  "   "    "     "    "   : ASSUME A LINE THROUGH THEM
C     3)- THREE POINTS "         "  "   "    "     "    "   : LINE FIT THROUGH POINTS
C     ENTER GEOMETRICAL INJECTION DIMENSIONS
      DIMENSION NG(3,18),RATIC(3,18),THETA(3),THETAO(18),ETADIA(18)
      DATA IYES/3HYES/
      DATA R,CP/287.,1148./
      TYPE 5
 5    FORMAT(' ENTER MAIN ORIFICE DIAMETER (MM)          : ',$)
      ACCEPT 10, ORDI
 10   FORMAT(F10.5)
      TYPE 6
 6    FORMAT(' ENTER BLEED ORIFICE DIAMETER (MM)         : ',$)
      READ(5,10) DIBL
      TYPE 7
 7    FORMAT(' ENTER INJECTION AREA (M**2)               : ',$)
      READ(5,10) ARIN
      TYPE 8
 8    FORMAT(' ENTER INJECTION HOLE DIAMETER(MM)         : ',$)
      READ(5,10) DHOI
      TYPE 9
 9    FORMAT(' ENTER INJECTION HOLE ANGLE(DEGREES)       : ',$)
      READ(5,10) ANGLE
C     ENTER INJECTION VARIABLES FROM EXPERIMENT
 210  TYPE 220
 220  FORMAT(' ENTER RUN NUMBER    ',$)
      READ(5,41) RUN
      WRITE(6,230)
      WRITE(6,240) RUN
 230  FORMAT('   RUN NUMBER  ')
 240  FORMAT(A10)
      ID=1
 3    CONTINUE
      TYPE 11
 11   FORMAT(' ENTER PLENUM TOTAL PRESSURE (BARS)        : ',$)
      READ(5,10) PLTOPR
      TYPE 12
 12   FORMAT(' ENTER PLENUM TOTAL TEMPERATURE(K)         : ',$)
      READ(5,10) TOPLEP
      TYPE 13
 13   FORMAT(' ENTER UPSTREAM ORIF. TOTAL PRESS (BARS)   : ',$)
      READ(5,10) UPTOPR
      TYPE 14
 14   FORMAT(' ENTER UPSTREAM ORIF. TOTAL TEMP (K)       : ',$)
      READ(5,10) TETOUP
      TYPE 15
 15   FORMAT(' ENTER ATMOSPHERIC PRESSURE (BARS)         : ',$)
      READ(5,10) ATPRE
      TYPE 16
 16   FORMAT(' ENTER   WALL  TEMPERATURE(K)              : ',$)
      READ(5,10) AMTE
      TYPE 21
```

```
21    FORMAT(' ENTER FREE STREAM MACH NUMBER             : ',$)
      READ(5,10) FSMACH
      TYPE 22
22    FORMAT(' ENTER FREE STREAM TOTAL PRESSURE(BARS)   : ',$)
      READ(5,10) RPOTST
      TYPE 23
23    FORMAT(' ENTER FREE STREAM TOTAL TEMPERATURE(K)   : ',$)
      READ(5,10) TOTEST
      TYPE 300
300   FORMAT('    YOU NEED H/HO VALUES  (YES/NO) ? ',$)
      READ(5,41) IRO
      IF(IRO.NE.IYES) GO TO 310
      DO 30 J=1,18
      TYPE 29
29    FORMAT(' ENTER GAGE NUMBER            : ',$)
      READ(5,31) NG(ID,J)
      TYPE 32
32    FORMAT(' ENTER H/HO RATIO VALUE       : ',$)
      READ(5,33) RATIO(ID,J)
30    CONTINUE
31    FORMAT(I3)
33    FORMAT(F10.5)
C     CALCULATION OF FREE STREAM STATIC PARAMETERS
310   TYPE 600
600   FORMAT(' CALCULATION OF ROCUC ISENTROPIC & ROINFUINF    ')
      VIVA=(1.+FSMACH**2/5.)
      EMFSST=TOTEST*VIVA**(-1.0)
      STFSPR=RPOTST*VIVA**(-7./2.)
      FSDENS=STFSPR*1.E5/R/EMFSST
      VLOV=SQRT(1.414*R*EMFSST)
      VELOFS=FSMACH*VLOV
      WRITE(6,800)
800   FORMAT(1X,'       FREE     STREAM          CONDITIONS       ')
      WRITE(6,820)
      WRITE(6,810) EMFSST,STFSPR,FSDENS,VELOFS
810   FORMAT(4E12.5)
820   FORMAT('     STATTEMP  STATPRE     DENSITY     VELOCITY    ')
C     CALCULATION OF ISENTROPIC MASS FLUX RATIO
      ALFA=PLTOPR/RPOTST
      BETA=(1.-(ALFA*RPOTST/STFSPR)**(-2./7.))
      GAMMA=(1.-(RPOTST/STFSPR)**(-2./7.))
      DELTA=SQRT(BETA/GAMMA)
      BLOWNG=ALFA**(2./7.)*(TOTEST/TOPLEP)**0.5*DELTA
      ZCOL=FSDENS*VELOFS
      CLIS=BLOWNG*ZCOL
      TYPE 40
40    FORMAT(' IS THE MAIN ORIFICE DIAMETER AVAILABLE(YES/NO)?',$)
      READ(5,41) IRO
41    FORMAT(   A10)
      IF(IRO.EQ.IYES) GO TO 43
      TYPE 42
42    FORMAT(' CALCULATION THROUGH CD   ')
      TYPE 35
35    FORMAT(' ENTER THE VALUE OF THE DISCHARGE COEFFICIENT :   ',$)
      READ(5,10) CD
      COOLAC=CD*CLIS
      GO TO 45
43    TYPE 44
44    FORMAT(' CALCULATION THROUGH MAIN ORIFICE DIAMETER   ')
C     CALCULATION OF MASS FLOW RATE THROUGH MAIN ORIFICE AND BLEEDS
C     AND OF THE INJECTION PARAMETERS
```

```
      PI=3.141592654*4.0424/1000./4.
      AMASS=PI*ORDI**2*UPTOPR/TETOUP**0.5
      BLEMA=PI*DIBL**2*PLTUPR/TOPLEP**0.5
      AIN=AMASS-2.*BLEMA
      COOLAC=AIN/ARIN
   45 SQUARE=SQRT((STFSPR*100000/R)**2+2.*COOLAC**2/CP*TOPLEP)
      SRE=(-(STFSPR*100000/R)+SQUARE)/COOLAC**2*CP
      OOO=COOLAC/ZCOL
      CODE=1./SRE
      CLOVE=COOLAC/CODE
      COSITE=TOPLEP-CLOVE**2/2./CP
      AMOFLU=CODE*CLOVE**2/FSDENS/VELOFS**2
      DENRAT=CODE/FSDENS
      THETA(ID)=(TOTEST-TOPLEP)/(TOTEST-AMTE)
      DC=COOLAC/CLIS
      WRITE(6,900)
      WRITE(6,901) CODE,CLOVE,COSTTE
  900 FORMAT(1X,'     COOLANT  STATIC   CONDITIONS   ')
  901 FORMAT(1X,3E14.5)
      VELRAT=CLOVE/VELOFS
      WRITE(6,99)
      WRITE(6,100) VELRAT,DENRAT,AMOFLU,COOLAC,THETA(ID),OOO,CDIS,CD,DC
  100 FORMAT(1X,9E10.3)
   99 FORMAT('  VELRATIO   DENSRAT   MOMRAT   RCUCAC   THETA   ',
     *'  MASSRAT  RCUCIS   CDASS    CDCALC  ')
      TYPE 46
   46 FORMAT(' DO YOU ASSUME HF/HO EQUAL TO 1 ?(YES/NO) ',$)
      READ(5,41) IRO
      IF(IRO.EQ.IYES) GO TO 50
      TYPE 47
   47 FORMAT(' TWO POINTS ON THE H/HO VS THETA PLOT?(YES/NO) ',$)
      READ(5,41) IRO
      IF(IRO.EQ.IYES) GO TO 54
      TYPE 48
   48 FORMAT(' THREE POINTS ON THE H/HO VS THETA PLOT?(YES/NO)',$)
      READ(5,41) IRO
      IF(IRO.EQ.IYES) GO TO 57
      TYPE 200
  200 FORMAT(' ARE YOU REDUCING A NEW RUN ?(YES/NO) ',$)
      READ(5,41) IRO
      IF(IRO.EQ.IYES) GO TO 210
      STOP
C     CALCULATION OF ADIABATIC FILM COOLING EFFECTIVENESS:FIRST OPTION
   50 DO 52 J=1,18
      THETAO(J)=THETA(ID)+RATIO(ID,J)*THETA(ID)/(1.-RATIO(ID,J))
   52 ETADIA(J)=1./THETAO(J)
      WRITE(6,102)
      WRITE(6,103) (ETADIA(J),J=1,18)
  102 FORMAT('      VALUES   OF  ETA   ADIABATIC      ')
  103 FORMAT(18F5.2)
      STOP
   54 IF(ID.EQ.2) GO TO 55
      ID=2
      GO TO 3
C     CALCULATION OF THE ADIABATIC FILM COOLING EFFECTIVENESS:2ND OPTION
   55 DO 56 J=1,18
      THETAO(J)=(THETA(2)-THETA(1))/(RATIO(2,J)-RATIO(1,J))
     *(-RATIO(1,J))+THETA(1)
   56 ETADIA(J)=1./THETAO(J)
      WRITE(6,102)
      WRITE(6,103) (ETADIA(J),J=1,18)

      STOP
   57 IF(ID.EQ.3) GO TO 58
      ID=ID+1
      GO TO 3
C     CALCULATION OF THE ADIABATIC FULM COOLING EFFECTIVENESS:3RD OPTION
   58 DO 60 J=1,18
      BFAC=(3.*(THETA(1)*RATIO(1,J)+THETA(2)*RATIO(2,J)+THETA(3)
     **RATIO(3,J))-(THETA(1)+THETA(2)+THETA(3))*(RATIO(1,J)+
     *RATIO(2,J)+RATIO(3,J)))/(3.*(THETA(1)**2+THETA(2)**2+THETA(3)
     ***2)-(THETA(1)+THETA(2)+THETA(3))**2)
      AFAC=((THETA(1)**2+THETA(2)**2+THETA(3)**2)*(RATIO(1,J)+
     *RATIO(2,J)+RATIO(3,J))-(THETA(1)+THETA(2)+THETA(3))*(THETA(1)
     **RATIO(1,J)+THETA(2)*RATIO(2,J)+THETA(3)*RATIO(3,J)))/(3.*
     *(THETA(1)**2+THETA(2)**2+THETA(3)**2)-(THETA(1)+THETA(2)+
     *THETA(3))**2)
      THETAO(J)=-AFAC/BFAC
   60 ETADIA(J)=1./THETAO(J)
      WRITE(6,102)
      WRITE(6,103)(ETADIA(J),J=1,18)
      STOP
      END
```

TEST	ρ_c	u_c	T_c	u_c/u_∞	ρ_c/ρ_∞	$\rho_c u_c^2 / \rho_\infty u_\infty^2$	$\rho_c u_c / \rho_\infty u_\infty$	$\rho_c u_{c_{is}}$	$\rho_c u_{c_a}$	$T_{o,c}$	α	ϑ	
388	2.67	121.33	287.49	.49	1.29	.31	.63	625	323	293.9	1.021	.98	
389	2.71	162.70	282.47	.65	1.31	.56	.86	761	441	294.0	1.157	.98	
390	2.73	179.10	280.73	.72	1.32	.69	.95	899	489	294.7	1.316	.97	
391	2.80	220.57	273.91	.89	1.36	1.07	1.20	1030	618	295.1	1.498	.97	
392	2.86	260.61	268.45	1.01	1.38	1.40	1.39	1140	717	295.8	1.686	.96	
393	2.92	274.84	262.70	1.11	1.41	1.72	1.56	1220	802	295.6	1.837	.96	
403	2.68	258.30	283.84	1.04	1.31	1.41	1.36	1050	693	312.9	1.590	.81	
404	2.62	233.00	290.75	.94	1.28	1.12	1.20	942	610	314.4	1.428	.79	
405	2.59	217.73	293.95	.87	1.27	.97	1.11	886	563	314.6	1.349	.79	
406	2.55	194.37	297.05	.78	1.25	.76	.98	801	496	313.5	1.238	.80	
407	2.56	161.10	301.00	.65	1.24	.52	.80	681	412	312.3	1.088	.81	
408	2.53	127.46	304.32	.51	1.22	.32	.63	573	322	311.4	.989	.82	
409	2.52	100.63	305.49	.40	1.22	.20	.49	440	254	309.9	.893	.83	
410	2.51	84.32	306.30	.34	1.22	.14	.41	371	211	309.4	.854	.84	

TABLE 1

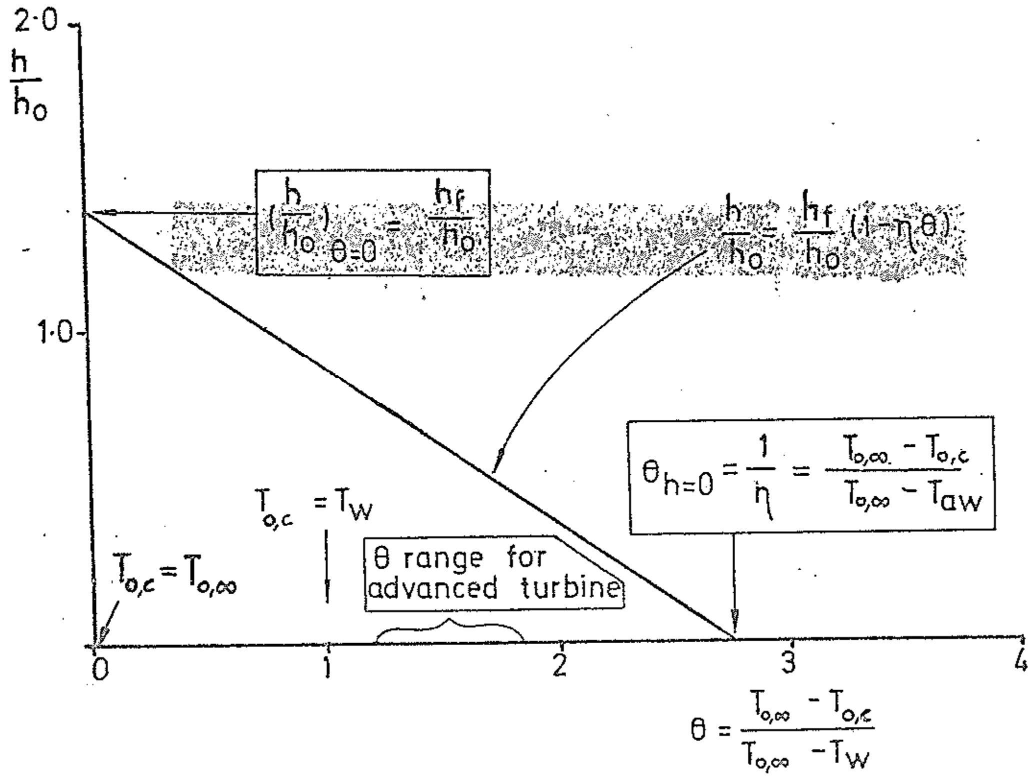

2·0
1·0
h/h_o
(h/h_o)_{θ=0} = h_f/h_o
h/h_o = h_f/h_o (1−η θ)
θ_{h=0} = 1/η = (T_{o,∞} − T_{o,c})/(T_{o,∞} − T_{aw})
T_{o,c} = T_W
T_{o,c} = T_{o,∞}
θ range for advanced turbine
0
1
2
3
4
θ = (T_{o,∞} − T_{o,c})/(T_{o,∞} − T_W)

Fig.1

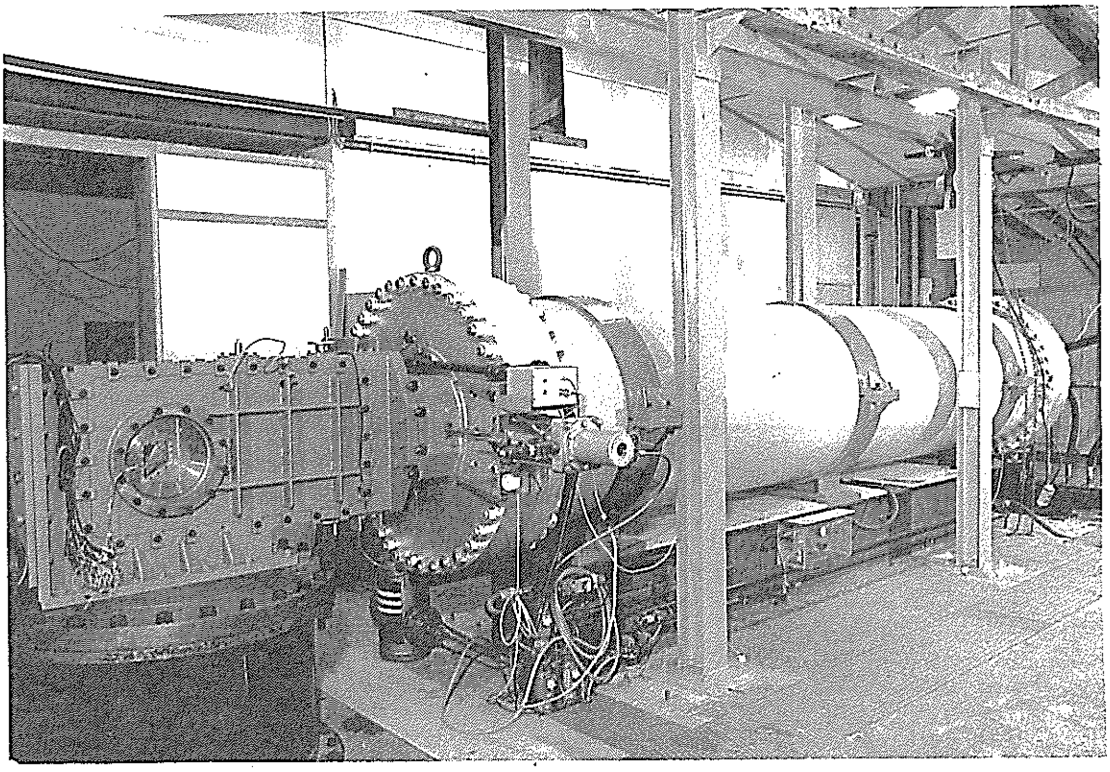

FIG. 2 - THE CT-2 HOT CASCADE FACILITY

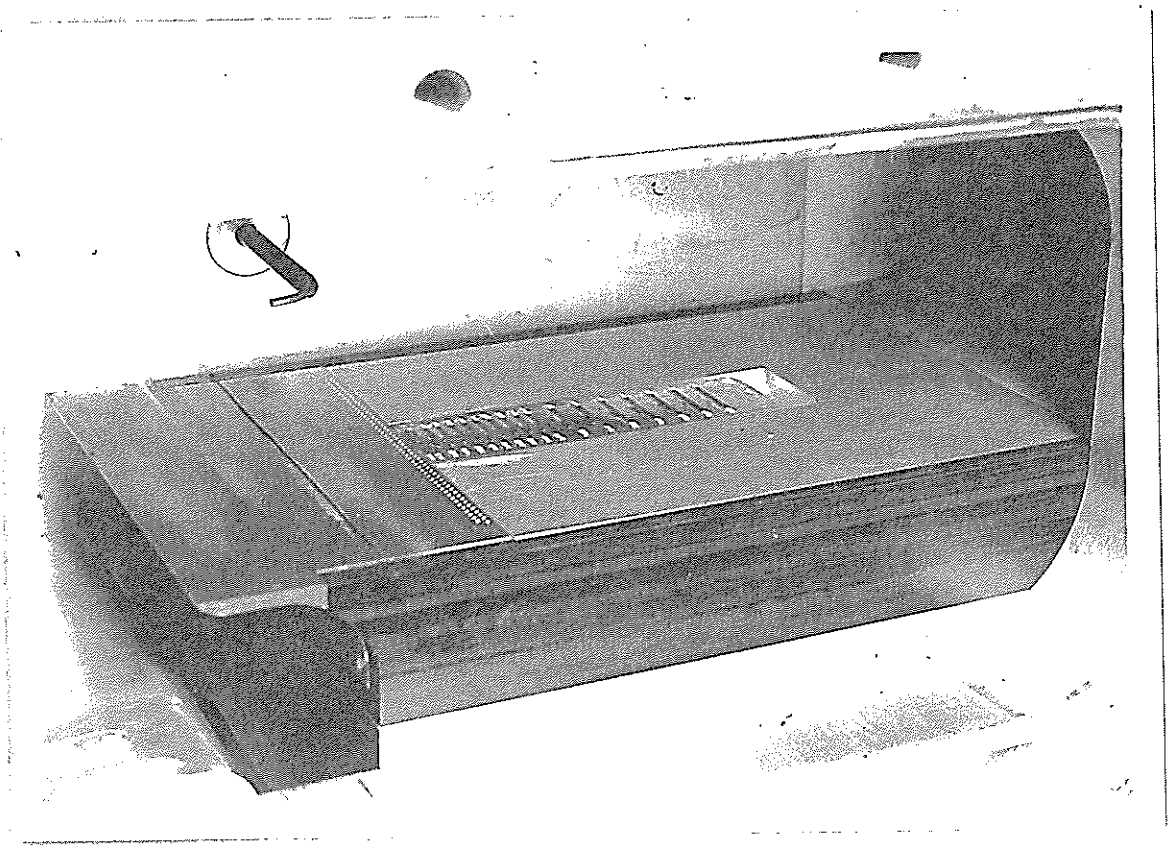

FIG. 3 - GENERAL VIEW OF THE INSTRUMENTED MODEL

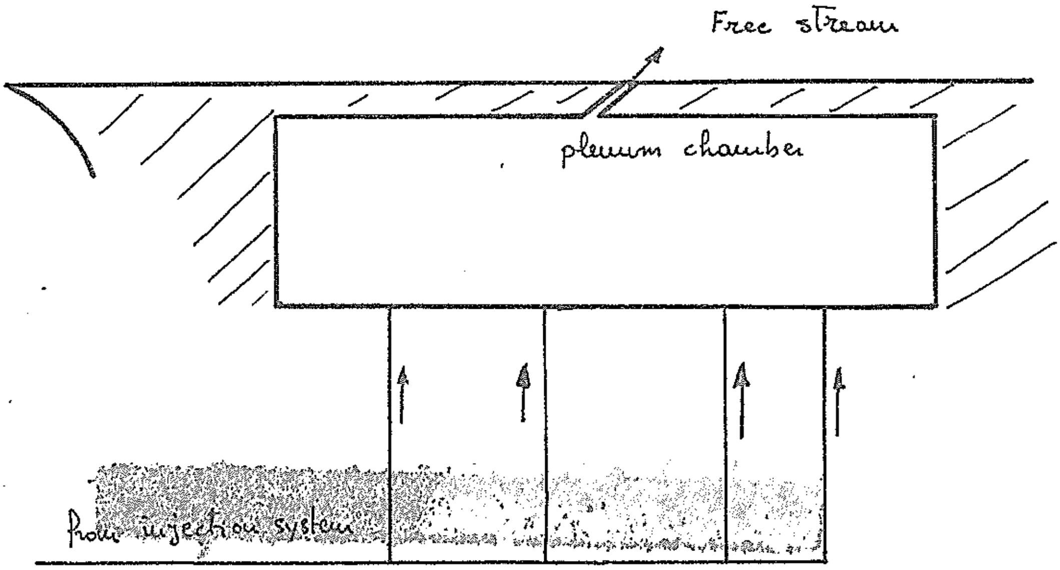
Free stream
plenum chamber
from injection system

Fig. 4

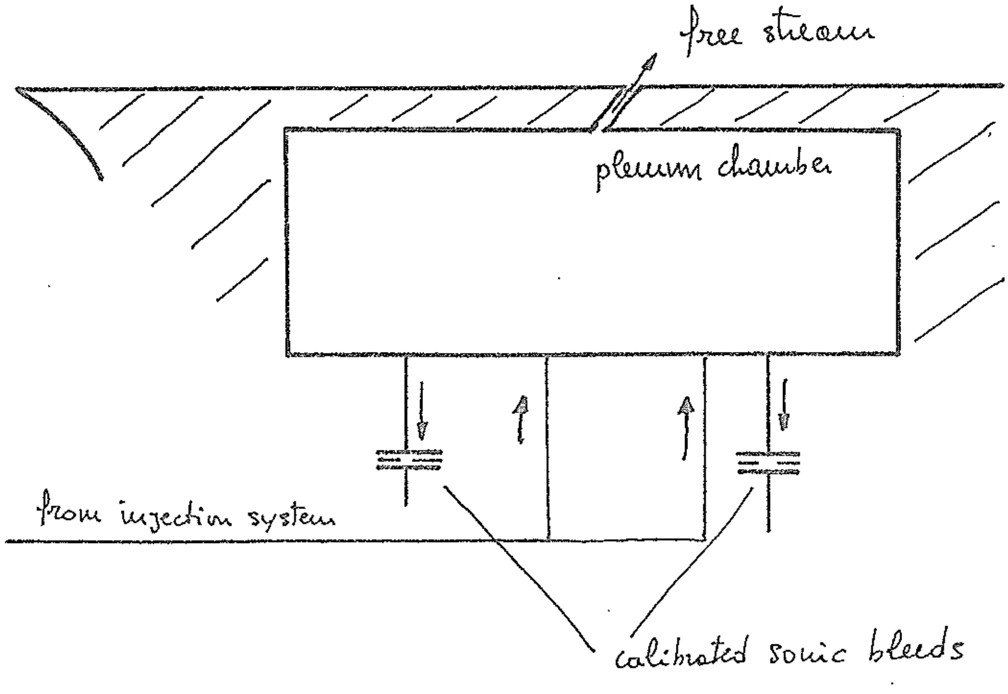
free stream
plenum chamber
from injection system
calibrated sonic bleeds

Fig. 5

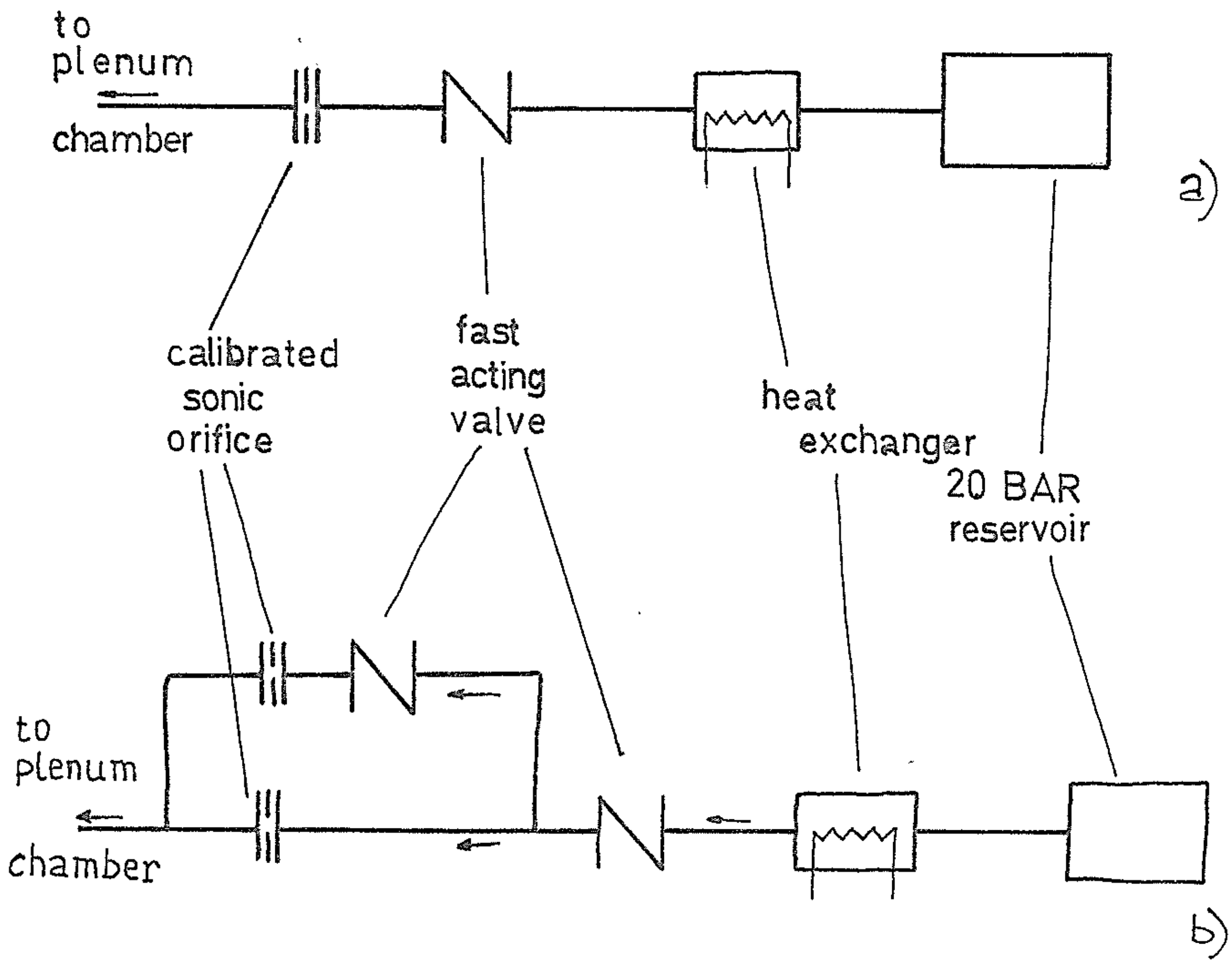
to
plenum
chamber
calibrated
sonic
orifice
fast
acting
valve
heat
exchanger
20 BAR
reservoir
a)
to
plenum
chamber
b)

Fig. 6

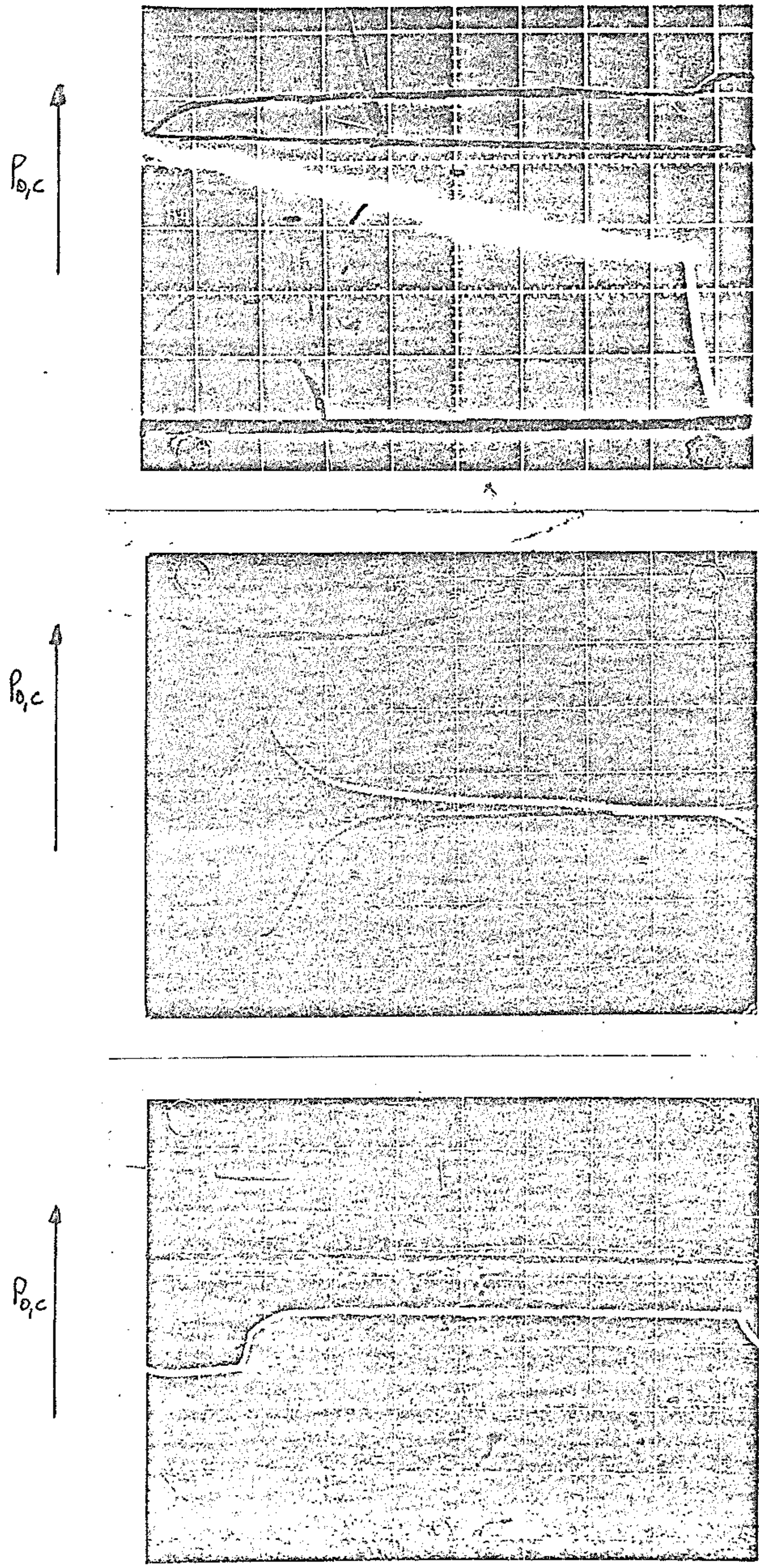

a) test 269

b) test 317

c) test 366

Fig 7 ⟶ time

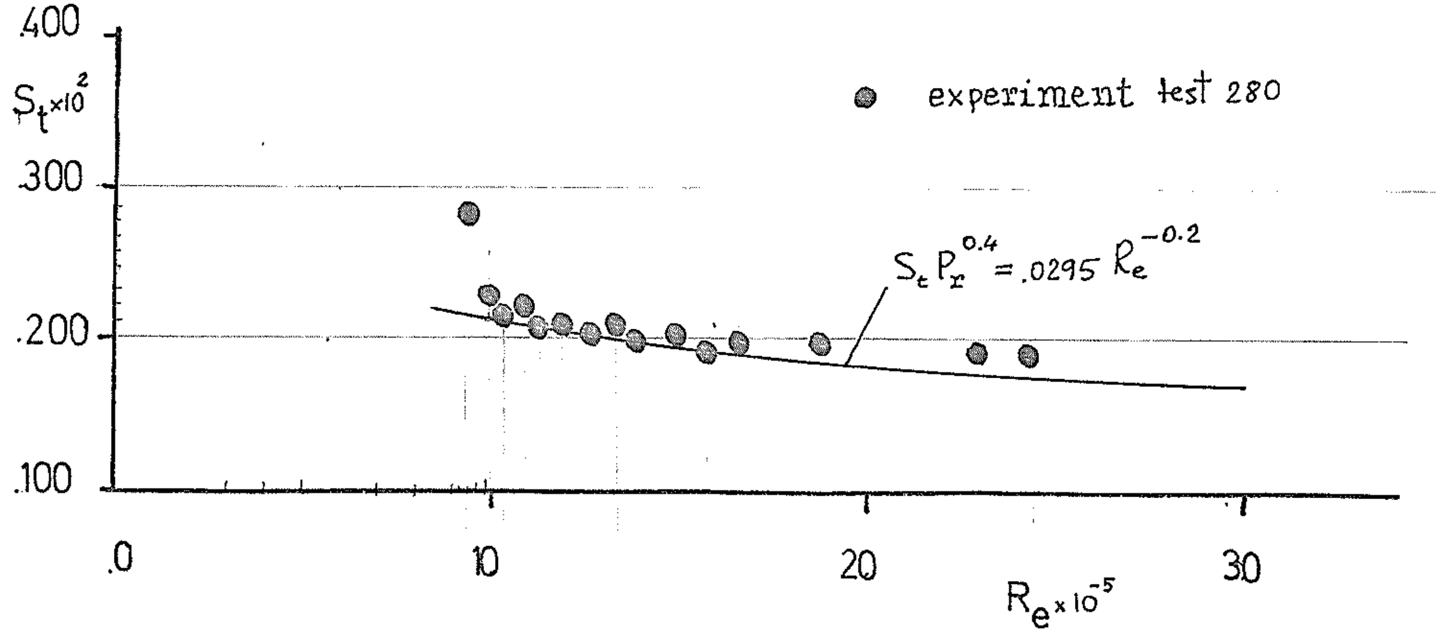

.400
$S_t \times 10^2$
.300
.200
.100
.0
10
20
30
$R_e \times 10^{-5}$
experiment test 280
$S_t P_r^{0.4} = .0295\, R_e^{-0.2}$

Fig. 8

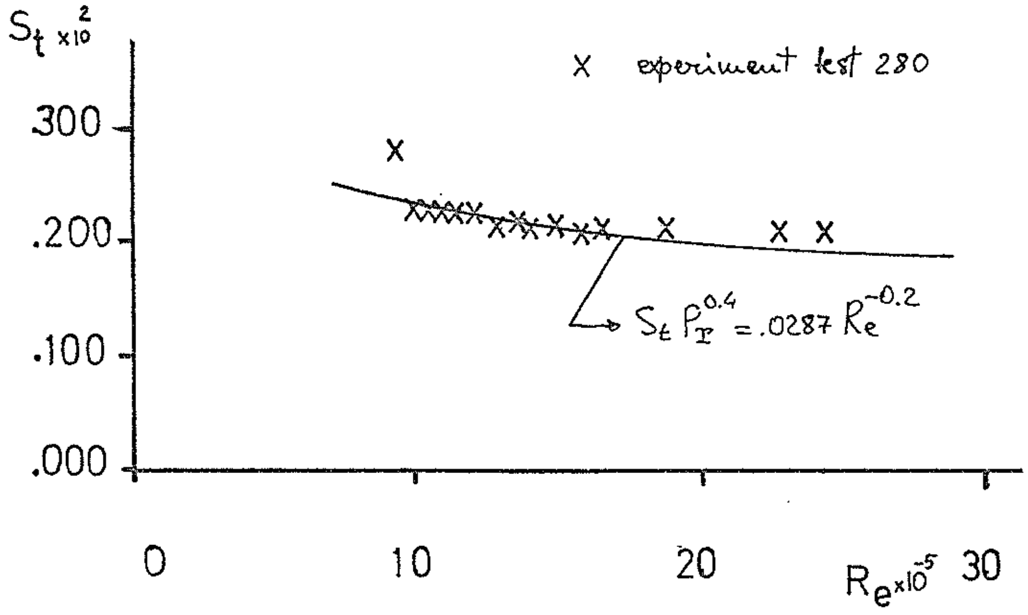

$S_t \times 10^2$
.300
.200
.100
.000
0
10
20
30
$R_e \times 10^{-5}$
X experiment test 280
$S_t P_r^{0.4} = .0287 R_e^{-0.2}$

Fig. 9

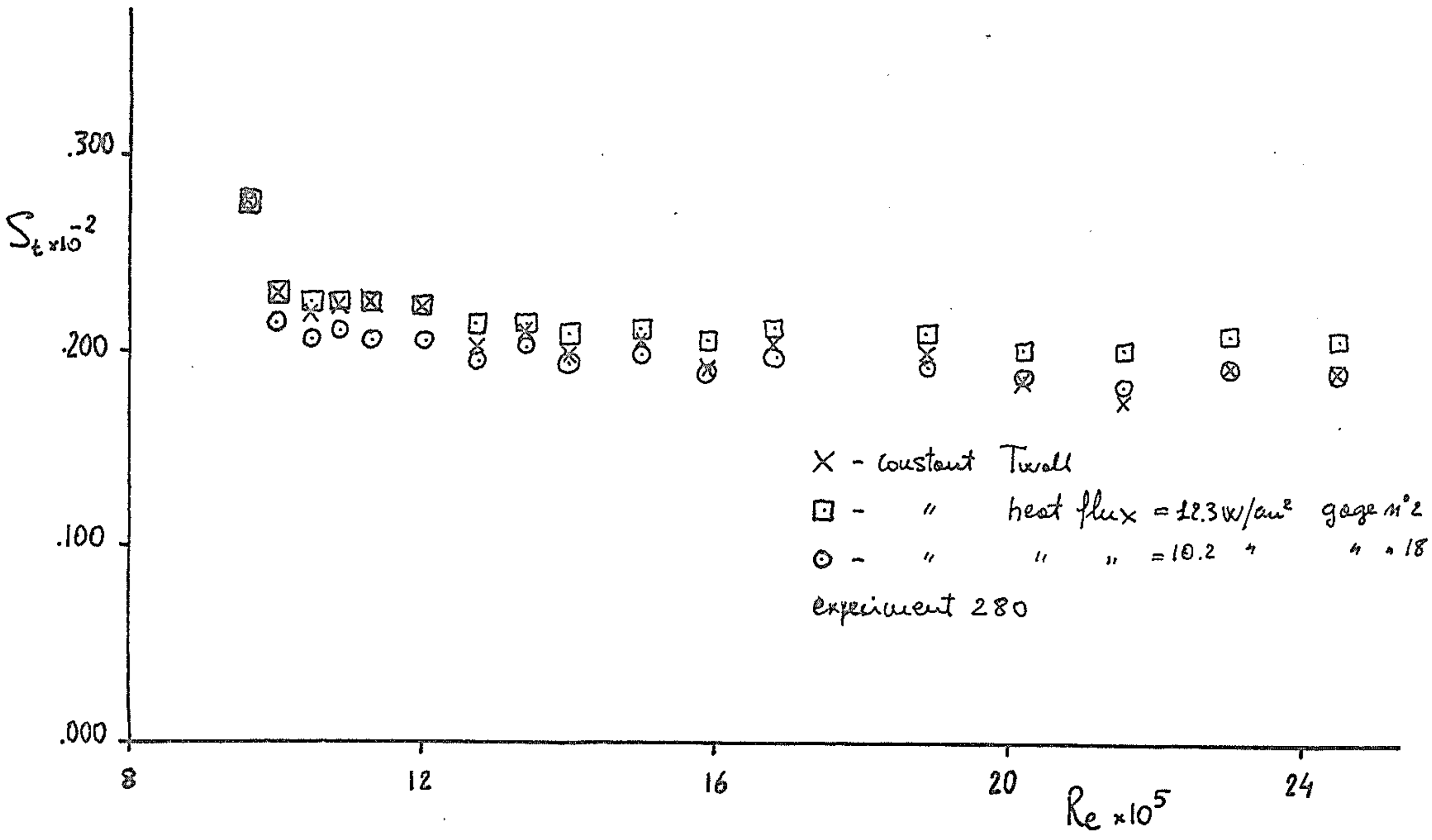

.300
.200
.100
.000
St ×10^-2
8
12
16
20
24
Re ×10^5
X - constant Twall
⊡ - " heat flux = 12.3 W/cm² gage n°2
⊙ - " " " = 10.2 " " n 18
experiment 280

Fig.. 10

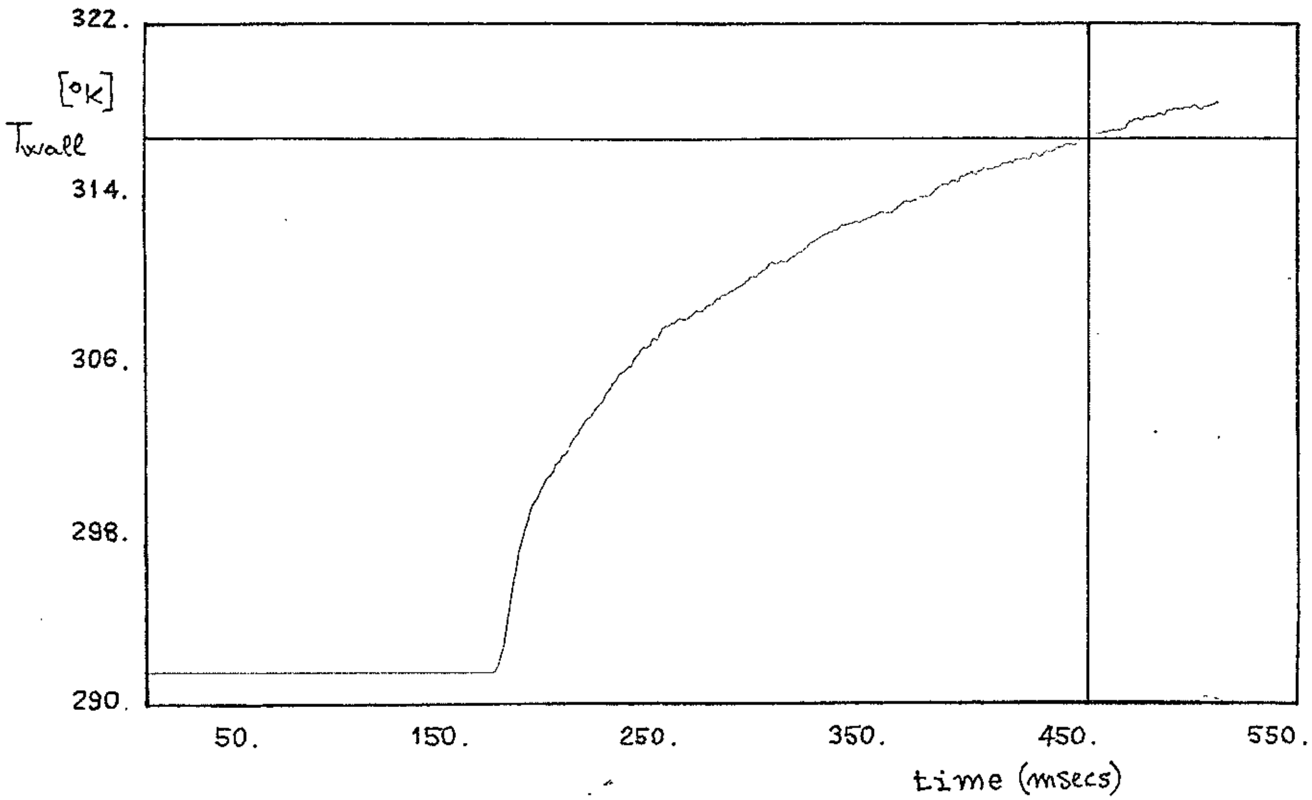

Fig 11

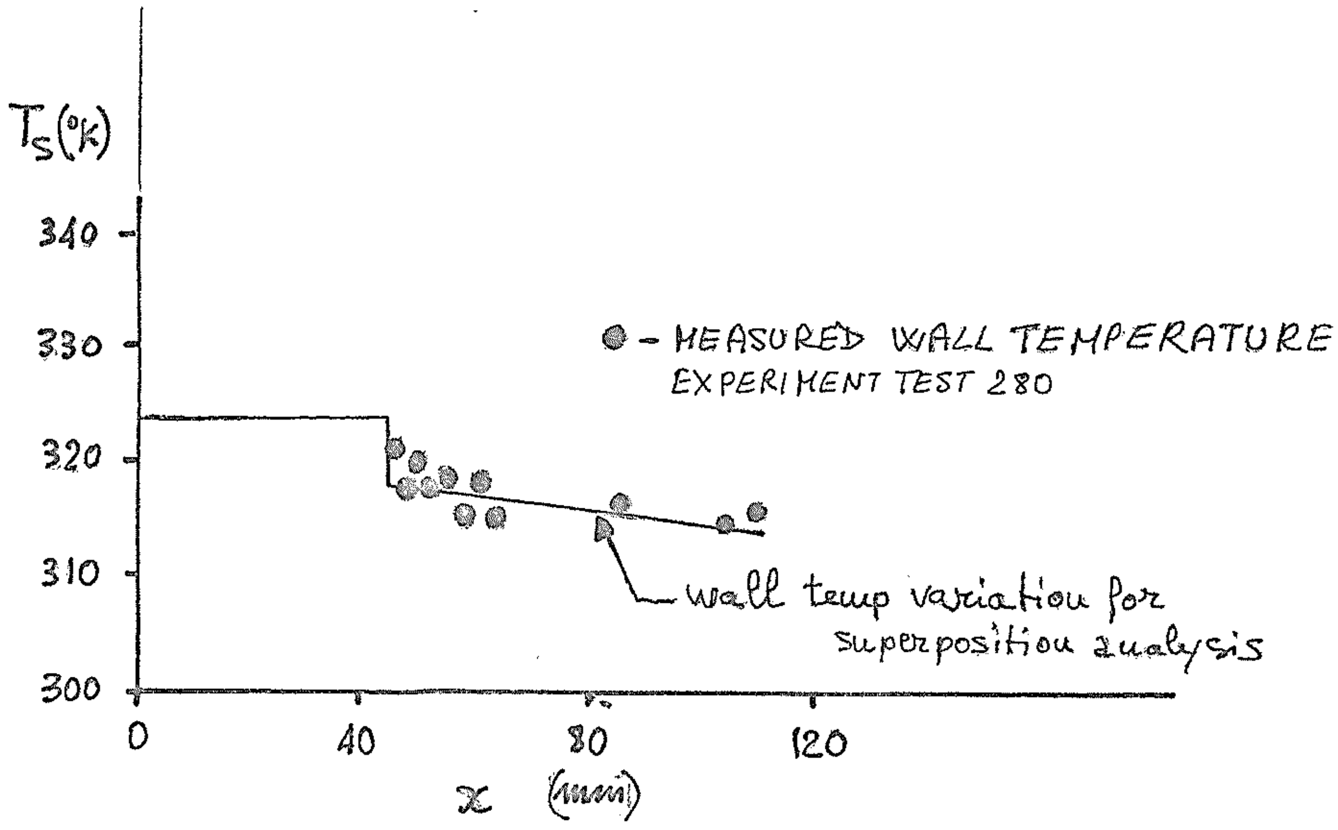

Ts(°K)
340
330
320
310
300
0
40
80
120
x (mm)
● - MEASURED WALL TEMPERATURE
EXPERIMENT TEST 280
wall temp variation for
superposition analysis

Fig. 12

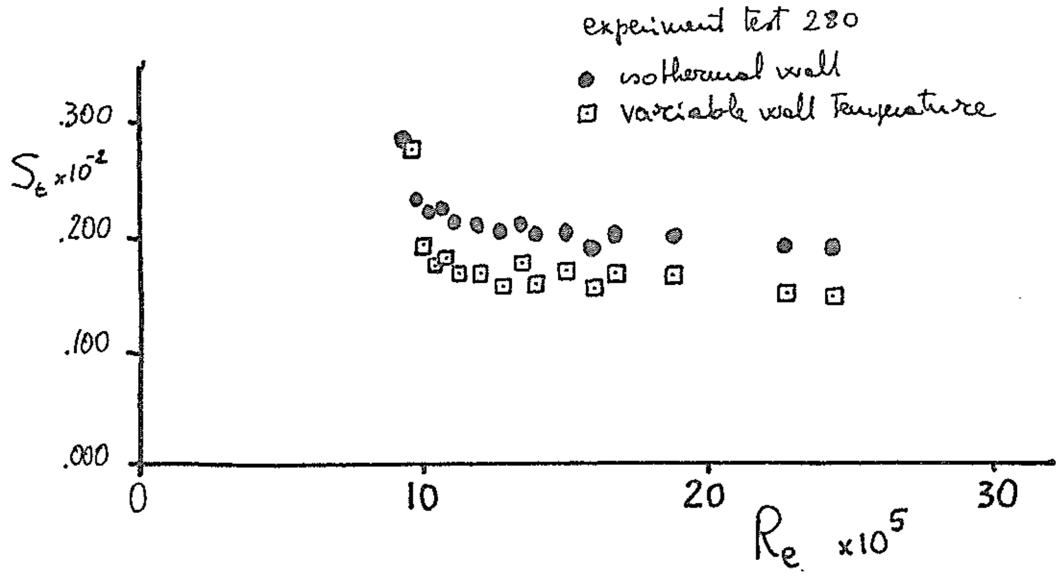
experiment test 280
isothermal wall
variable wall temperature
.300
.200
.100
.000
$S_t \times 10^{-2}$
0
10
20
30
$R_e \times 10^5$

Fig. 13

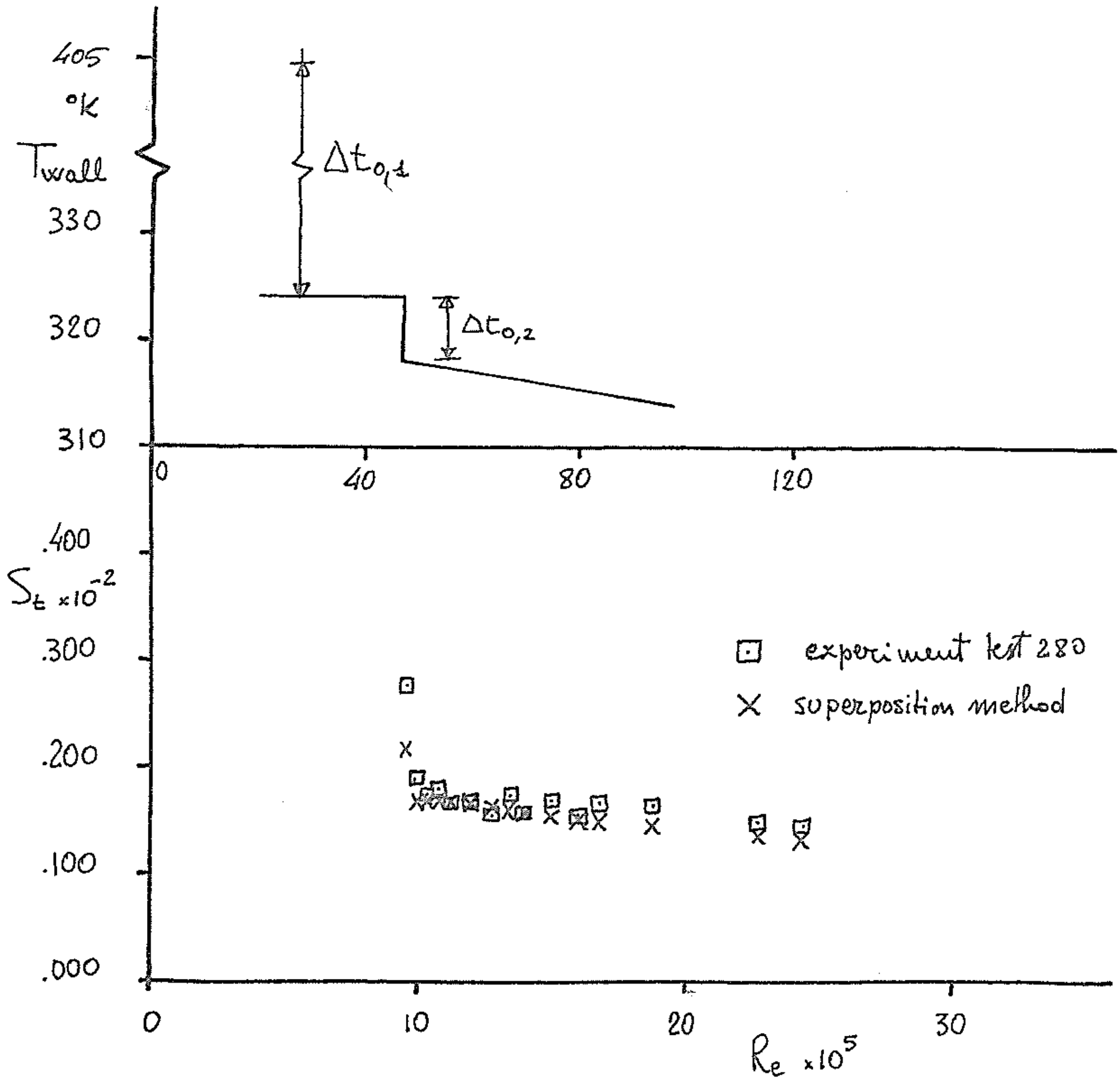
405
°K
Twall
330
320
310
$\Delta t_{0,1}$
$\Delta t_{0,2}$
0
40
80
120
.400
$S_t \times 10^{-2}$
.300
.200
.100
.000
experiment test 280
superposition method
0
10
20
30
$R_e \times 10^5$

Fig. 14

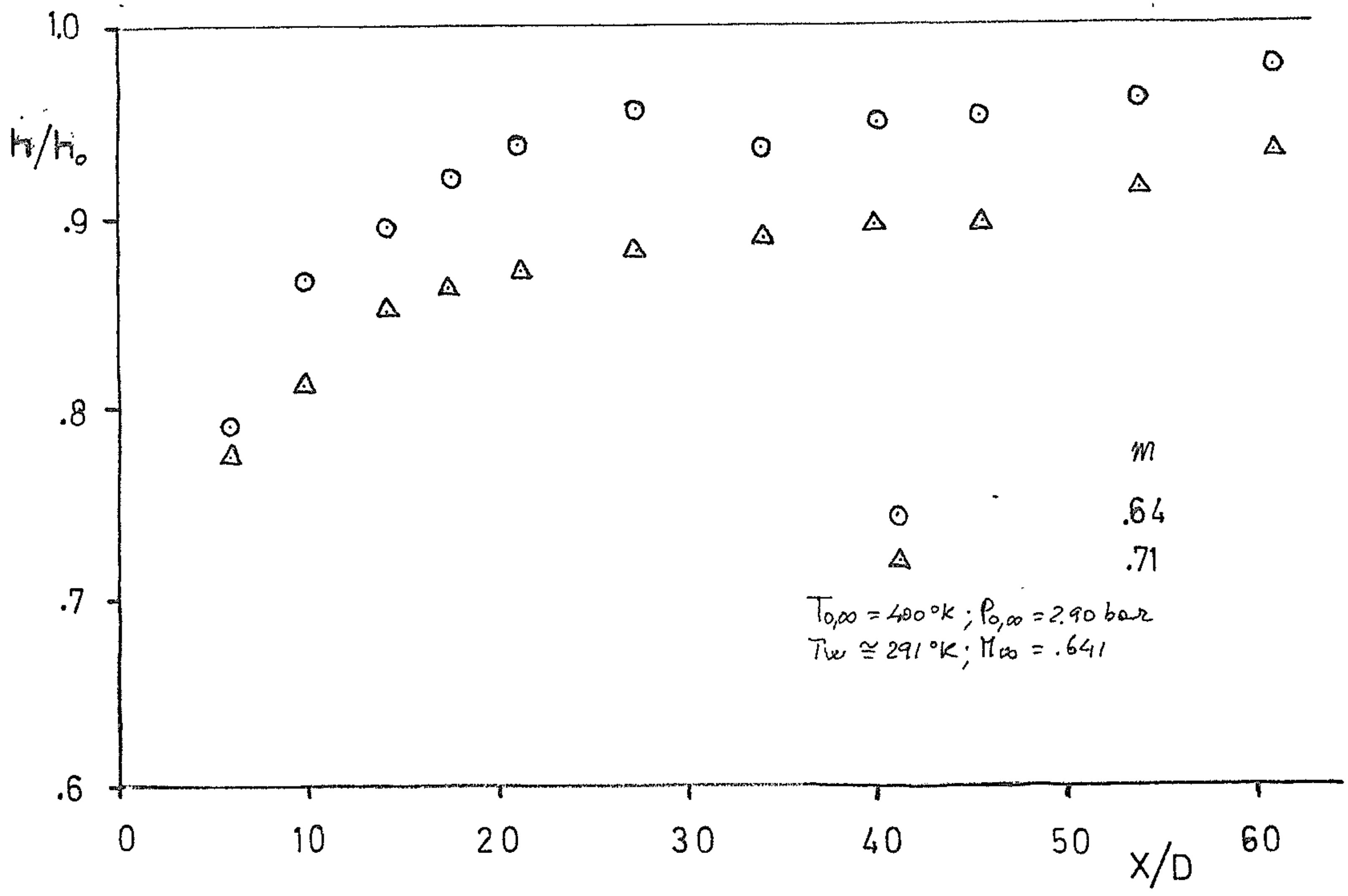
h/h_o
1.0
.9
.8
.7
.6
0
10
20
30
40
50
60
X/D
m
.64
.71
$T_{o,\infty} = 400\,°K\ ;\ P_{o,\infty} = 2.90$ bar
$T_w \cong 291\,°K\ ;\ M_\infty = .641$

Fig. 15

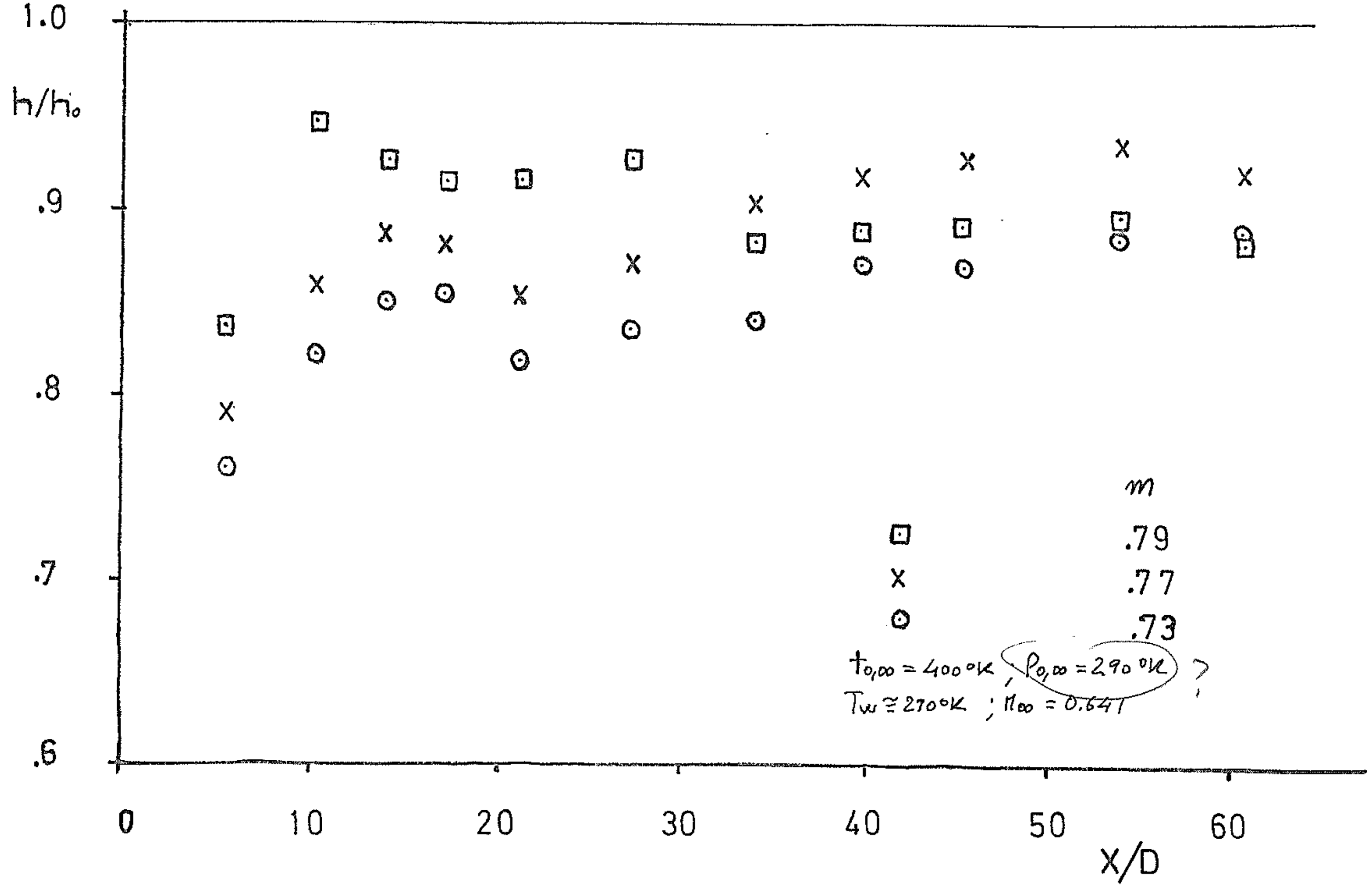
1.0
h/h₀
.9
.8
.7
.6
0
10
20
30
40
50
60
X/D
m
.79
.77
.73
$t_{0,\infty} = 400°K$, $p_{0,\infty} = 290°K$?
$T_w \cong 270°K$; $M_\infty = 0.641$

Fig. 16

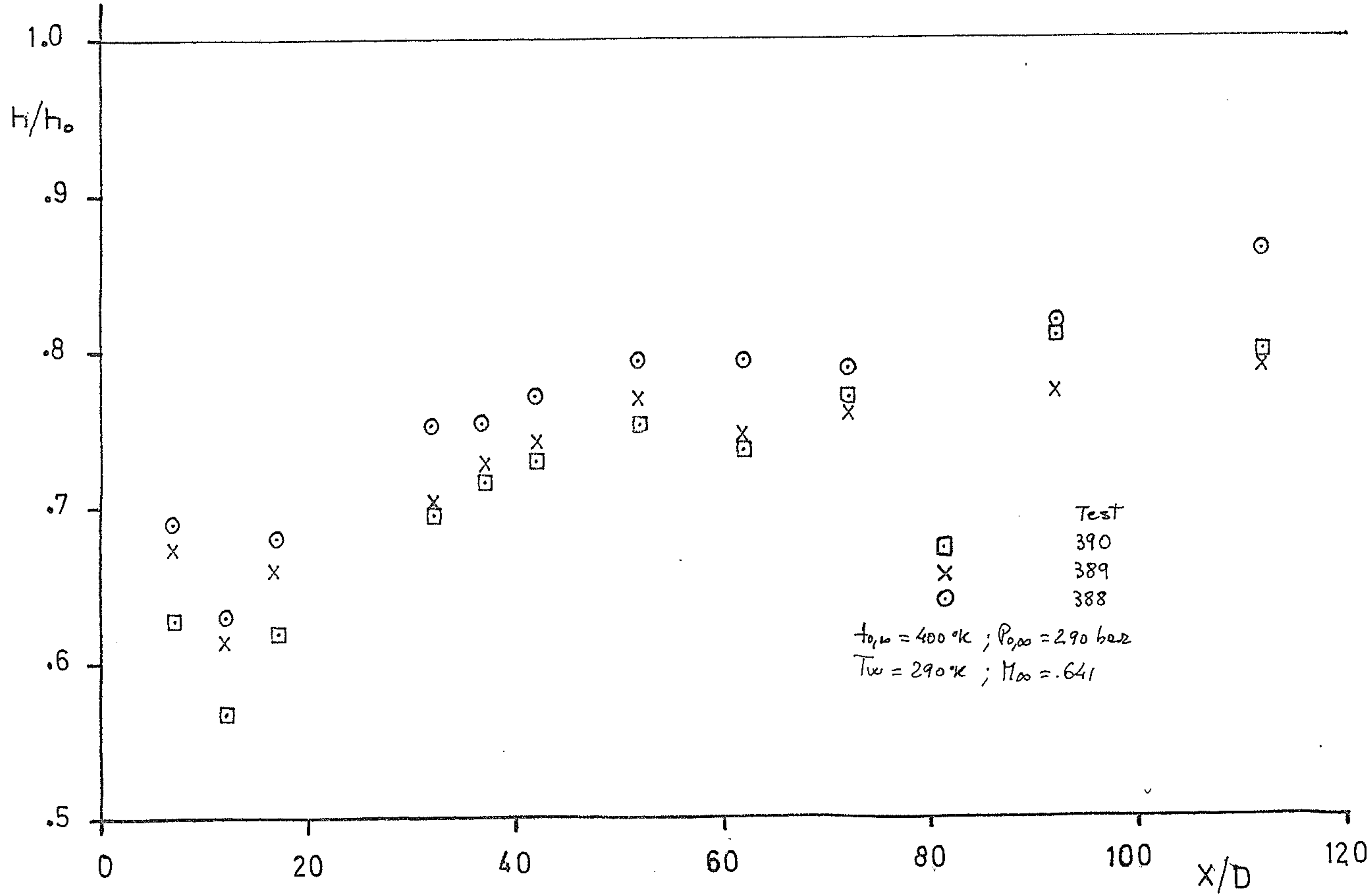

1.0
h_i/h_o
.9
.8
.7
.6
.5
0
20
40
60
80
100
120
X/D
Test
390
389
388
$t_{0,\infty} = 400\,°K$; $P_{0,\infty} = 2.90$ bar
$T_w = 290\,°K$; $M_\infty = .641$

Fig. 17

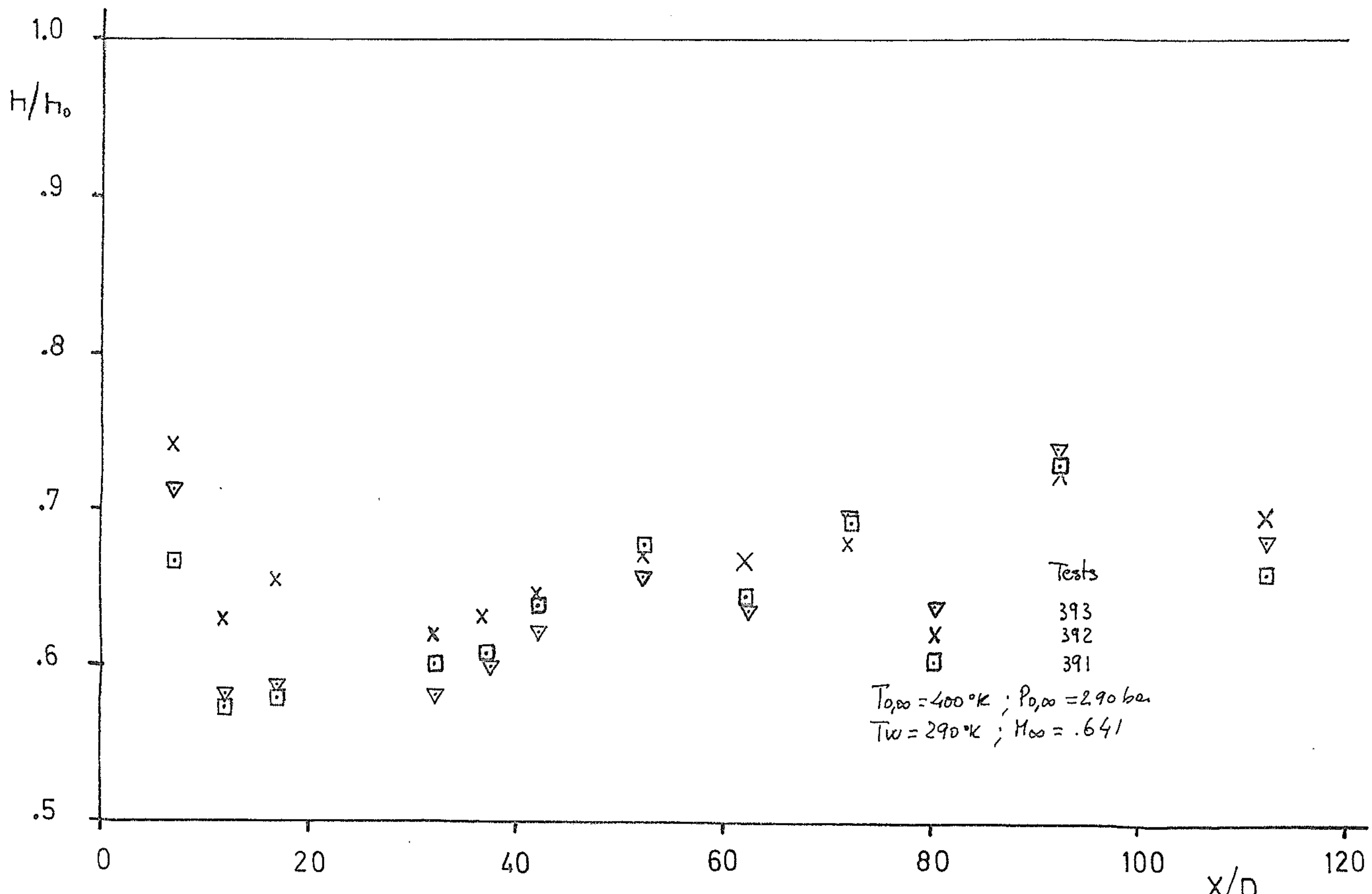
1.0
h/h₀
.9
.8
.7
.6
.5
0
20
40
60
80
100
120
X/D
Tests
393
392
391
$T_{0,\infty} = 400°K$; $P_{0,\infty} = 2.90$ bar
$T_w = 290°K$; $M_\infty = .641$

Fig. 18

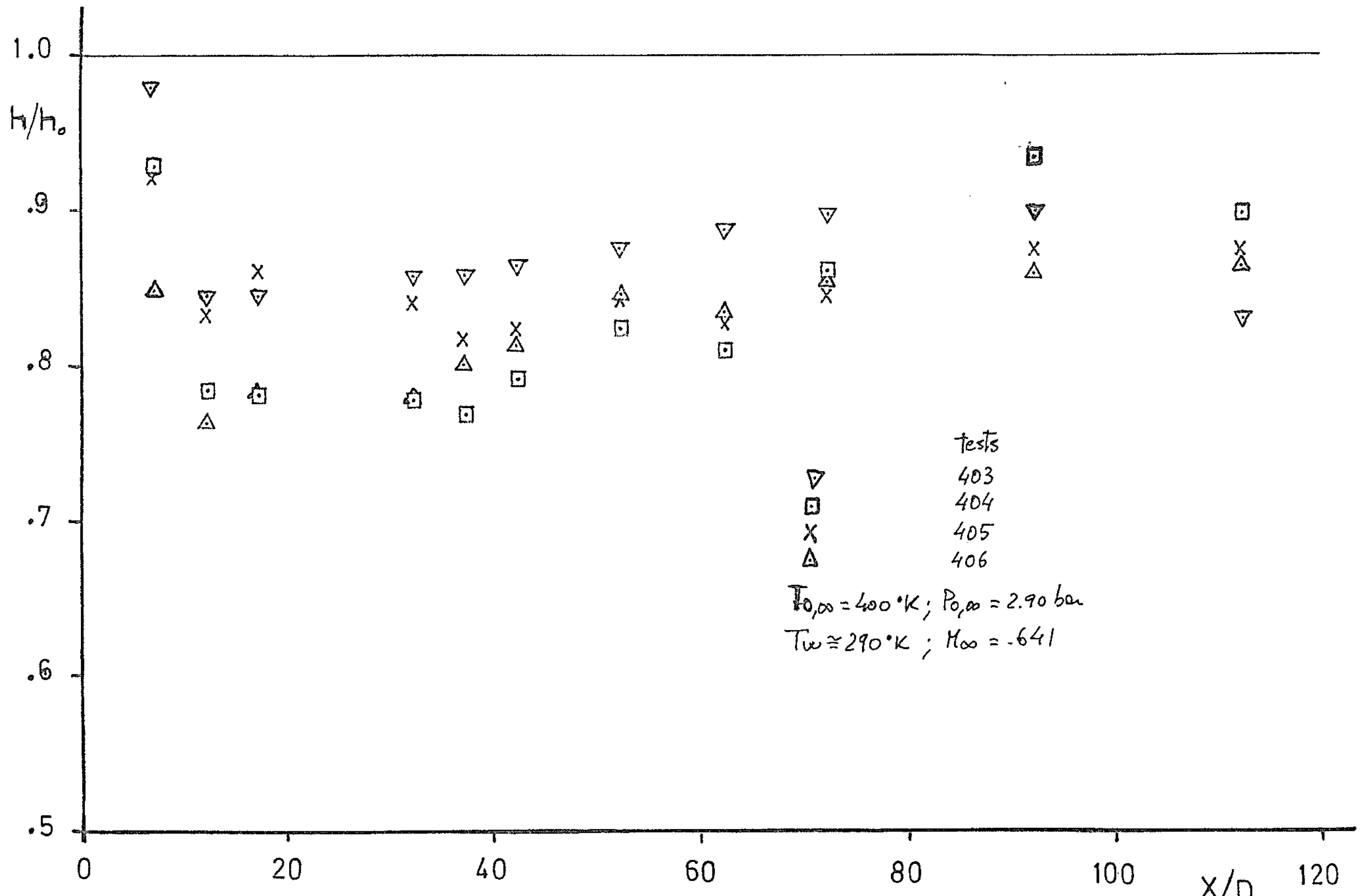

1.0
.9
.8
.7
.6
.5
h/h₀
0
20
40
60
80
100
120
X/D
tests
403
404
405
406
$T_{0,\infty} = 400\,°K$; $P_{0,\infty} = 2.90$ bar
$T_w \cong 290\,°K$; $M_\infty = .641$

Fig. 19

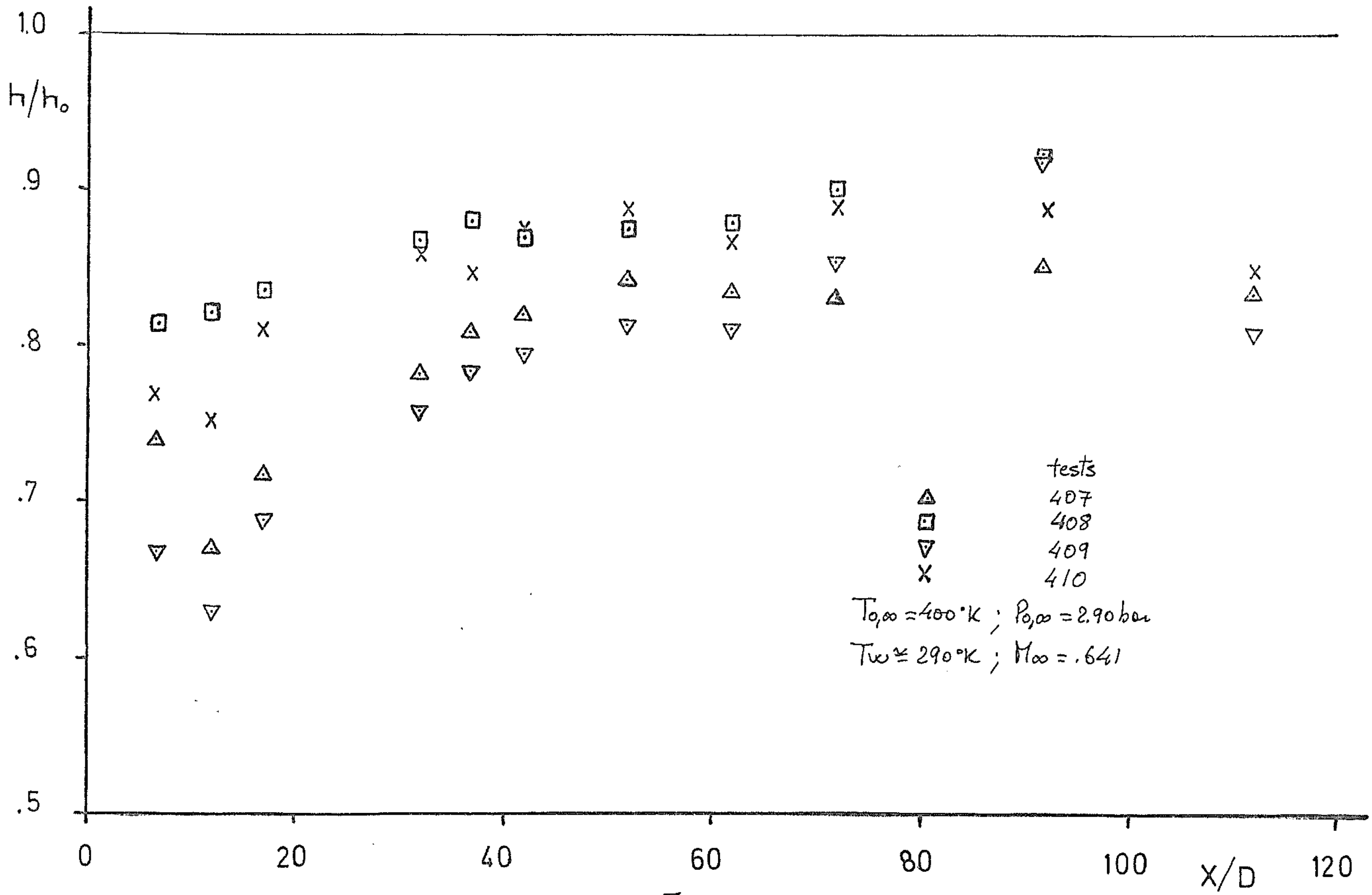

1.0
h/h₀
.9
.8
.7
.6
.5
0
20
40
60
80
100
120
X/D
tests
407
408
409
410
$T_{0,\infty} = 400°K$; $P_{0,\infty} = 2.90$ bar
$T_w \cong 290°K$; $M_\infty = .641$

Fig. 20

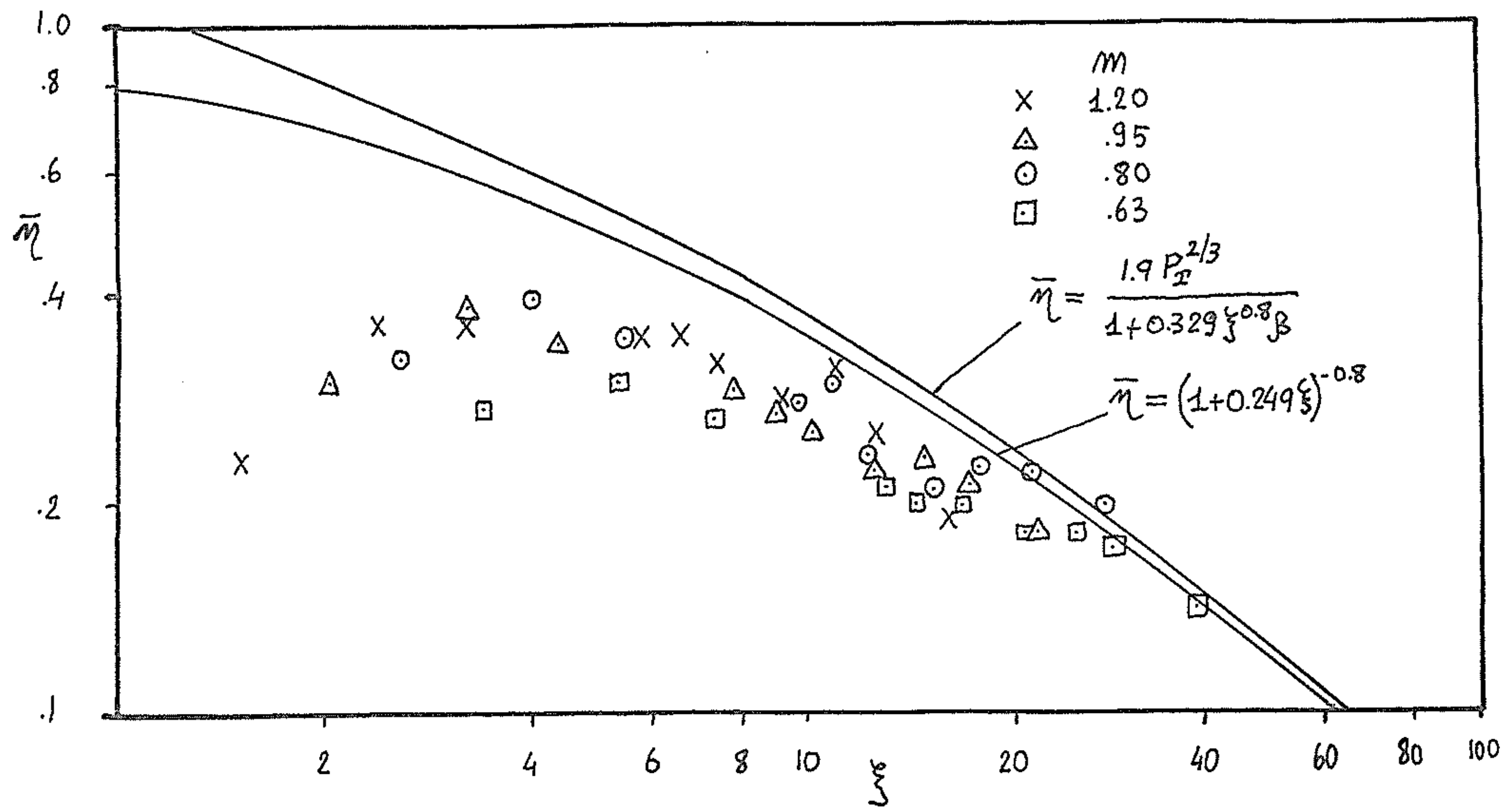

m
1.20
.95
.80
.63
$\bar{\eta} = \frac{1.9 P_{\mathrm{II}}^{2/3}}{1+0.329\xi^{0.8}\beta}$
$\bar{\eta} = (1+0.249\xi)^{-0.8}$
1.0
.8
.6
$\bar{\eta}$
.4
.2
.1
2
4
6
8
10
20
40
60
80
100
ξ

Fig. 22

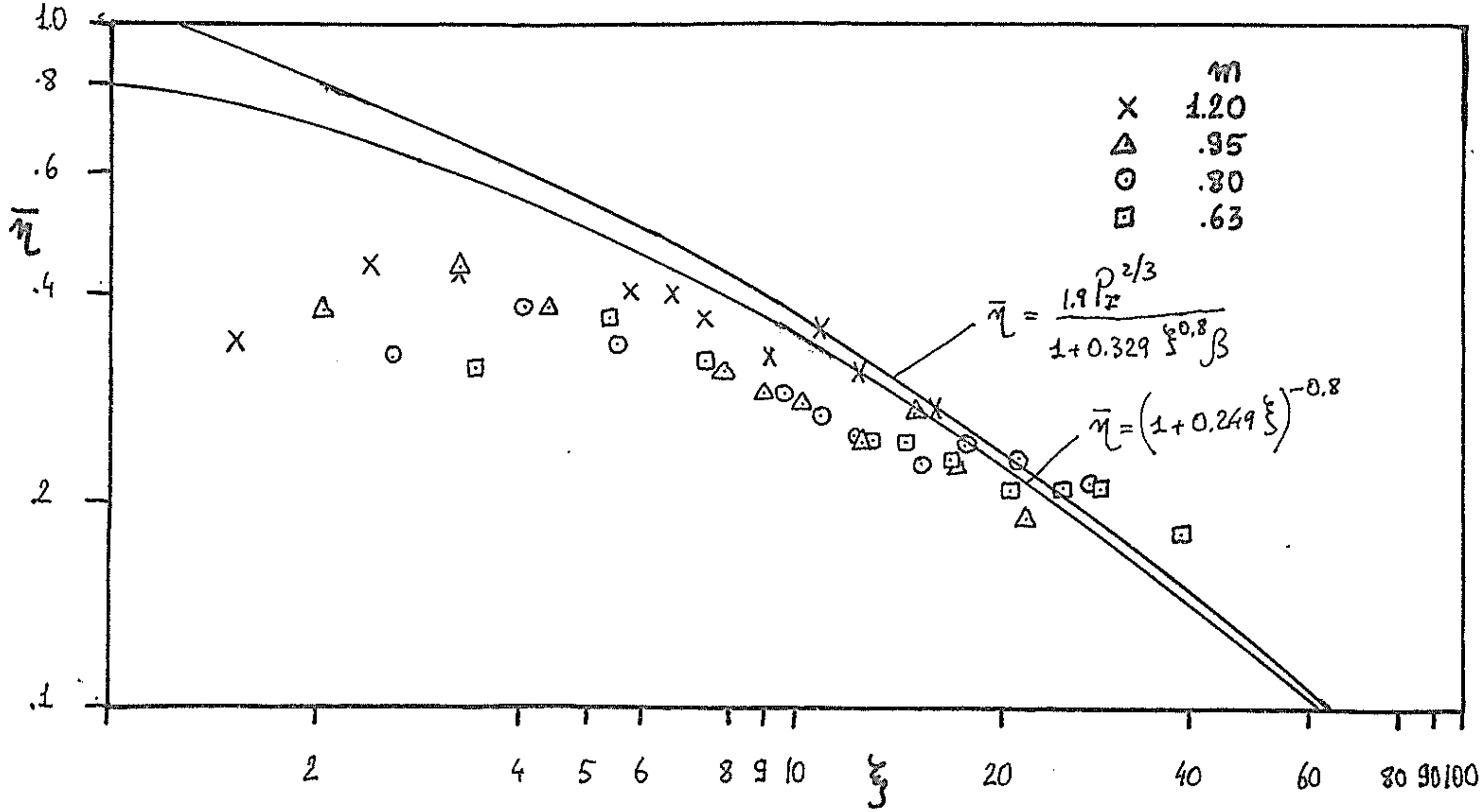

m
1.20
.95
.80
.63
$\bar{\eta} = \frac{1.9 P_r^{2/3}}{1+0.329\,\xi^{0.8}\beta}$
$\bar{\eta} = (1+0.249\,\xi)^{-0.8}$
1.0
.8
.6
.4
.2
.1
$\bar{\eta}$
2
4
5
6
8
9
10
20
40
60
80
90
100
ξ

Fig 22

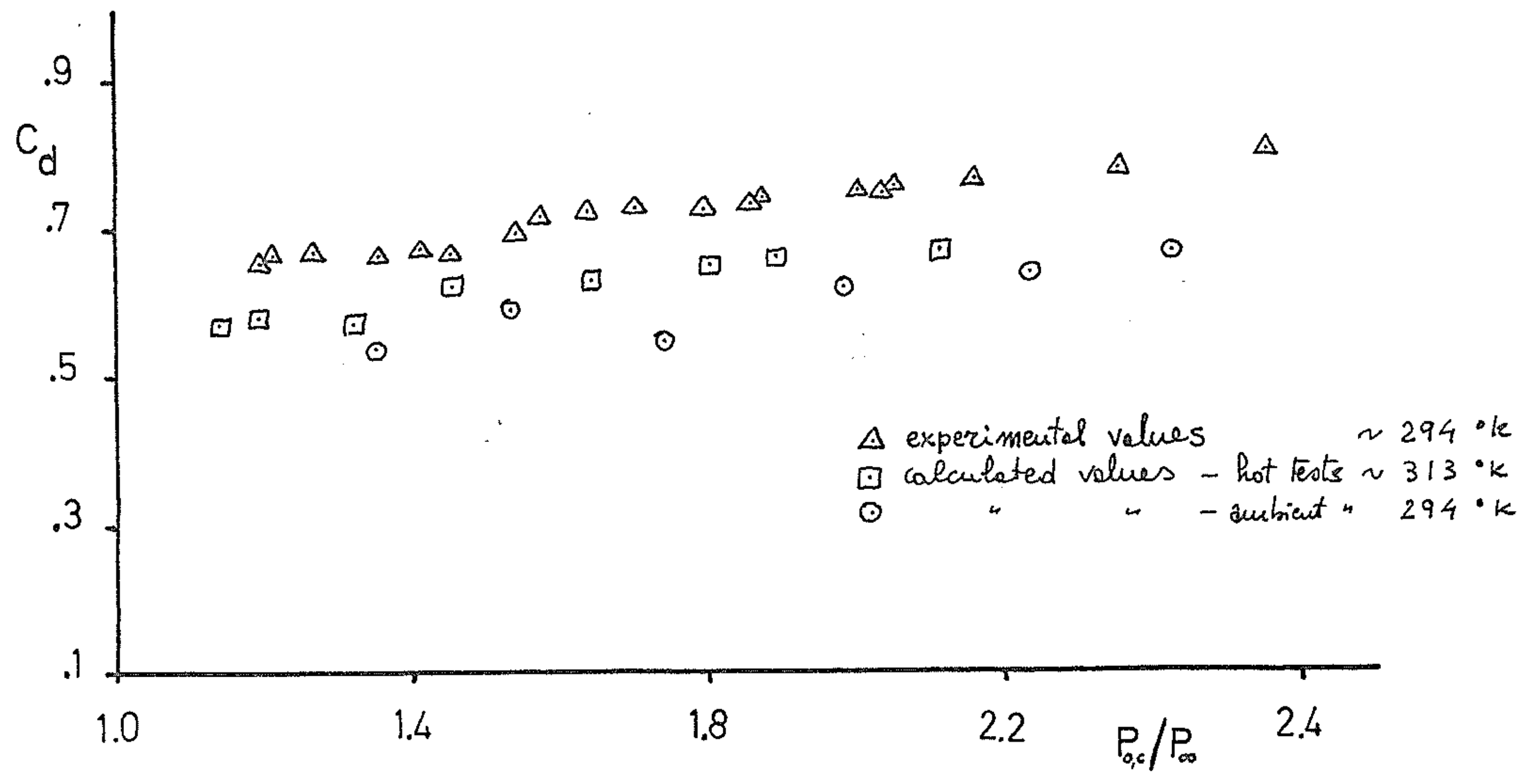

.9
.7
.5
.3
.1
C_d
1.0
1.4
1.8
2.2
2.4
$P_{o,c}/P_\infty$
experimental values ~ 294 °K
calculated values – hot tests ~ 313 °K
" " – ambient " 294 °K

Fig. 23